

### **Photocopy and Use Authorization**

In presenting this thesis in partial fulfillment of the requirements for an advanced degree at Idaho State University, I agree that the library shall make it freely available for inspection. I further state that permission for extensive copying of my thesis for scholarly purposes may be granted by the Dean of the Graduate School, Dean of my academic division, or by the University Librarian. It is understood that any copying or publication of this thesis for financial gain shall not be allowed without my written permission.

Signature \_\_\_\_\_

Date \_\_\_\_\_

Copyright (2021) Vincent Akula

A Numerical Study on The Effect of Changes to Air Distribution on Heating

Performance of a Forced Air Circulation System

by

Vincent Akula

A thesis

submitted in partial fulfillment

of the requirements for the degree of

Master of Science in the Department of Mechanical Engineering

Idaho State University

Fall 2021

To the Graduate Faculty:

The members of the committee appointed to examine the thesis of VINCENT AKULA find it satisfactory and recommend that it be accepted.

---

Anish Sebastian  
Major Advisor

---

Ken Bosworth  
Committee Member

---

Chikashi Sato  
Graduate Faculty Representative

## Table of Contents

Abstract .....	v
1 Introduction .....	1
1.1 Energy for Heating Spaces .....	1
1.2 Human Comfort in the Winter Season .....	2
1.3 Challenges of Heating Spaces in the Winter .....	3
2 Building Model.....	4
2.1 Building Codes .....	4
2.2 Residential Building Codes .....	4
2.3 Building Sample .....	5
2.4 Standard External/Internal Conditions .....	5
2.5 Building Heating Load Assessment .....	6
2.6 Forced Air Circulation Systems .....	8
2.7 Building Thermal System.....	8
3 Methodology.....	13
3.1 SimScale Dashboard .....	13
3.1.1 Creating a New Simulation Project .....	13
3.1.2 Importing the CAD Model .....	14
3.1.3 Flow Volume Extraction .....	14
3.1.4 Topological Sets .....	15
3.1.5 Creating the Simulation.....	16
3.1.6 Global Settings .....	17
3.1.7 Thermal Comfort Assessment .....	19
3.1.8 Simscale Meshing .....	20
3.1.9 OpenFOAM®.....	21
3.1.10 Setting up the simulation .....	22
3.2 Experiment Setup .....	23
3.2.1 Baseline Control Volume .....	23
3.2.2 Materials .....	25
3.2.3 Baseline Parameters.....	26
3.2.4 Boundary Conditions.....	26
3.2.4.1 Adiabatic Wall Boundary condition .....	28

3.2.4.2	External Wall Boundary condition .....	29
4	Results and Discussions.....	40
4.1	Air Vent Location Performance .....	40
4.2	Inlet Air Velocity Performance .....	43
4.3	Air Flow Rate Performance.....	45
4.4	The Local Mean Age of Air .....	55
4.5	Thermal Comfort Performance .....	55
4.6	Conclusions .....	56
4.7	Future Work .....	57
	References.....	58
	Appendix A: Standard Window Dimensions.....	63
	Appendix B: Standard Patio Door Dimensions .....	65
	Appendix C: Standard Entry Door Dimensions.....	68

# **A Numerical Study on The Effect of Changes to Air Distribution on Heating Performance of a Forced Air Circulation System**

## **Thesis Abstract – Idaho State University (2021)**

There is a potential to reduce residential energy consumption by harnessing “accessible and cost-effective technologies” such as a highly efficient heating system. In this study, Computational Fluid Dynamics (CFD) simulation is carried out on the baseline and modified versions of the baseline residential building’s heating system. The results are compared to investigate optimization opportunities. The modifications were limited to a specified room which included changing the location of air vents, the size of the air vents and the air flowrate. Performance criteria for the models included ASHRAE’s thermal comfort assessment, freshness of air using Simscale’s passive scalar source tool, heating efficiency, temperature distribution and air velocity efficiency. The results show that models with a higher air supply vents performed better particularly for thermal comfort and air velocity efficiency while lower air supply register models performed better for temperature distribution and heating efficiency. The models which showed better performance for heating and temperature distribution did not meet standards for thermal comfort, but the results provide a roadmap for innovative energy-efficient residential heating systems design.

### **Keywords**

Forced Air circulation, Heating performance, Air distribution, Residential building, heat flow in a room, temperature distribution,

# 1 Introduction

## 1.1 Energy for Heating Spaces

Heating and cooling buildings constitutes a major component of energy consumption in the U.S. According to the International Energy Agency (EIA), as of 2014, at least 76% of all U.S. electricity consumption and more than 40% of all U.S. energy consumed were expended on buildings (U.S. Energy Information Administration, 2014, p. MT5-17). Also, about 70% of buildings' total energy consumption in cold climates was for space heating and appliances; 45% of the total energy consumed was expended on heating spaces alone. In a recent release, for U.S., EIA reports also highlight a consistent spike in electricity usage in residential homes during the winter months of January and February. A similar increase can also be observed for the summer months of June, July and August. (U.S. Energy Information Administration, 2021, p. 143).

Table 1. Electricity End Use in the US for Jan 2019 – Nov 2020 (U.S. Energy Information Administration, 2021)

	All Values in Million KiloWattHours	Residential	% of Total	Commercial	% of Total	Industrial	% of Total	Total End Use
2019	January.....	133,318.....	39.1%	112,012.....	32.8%	82,610.....	24.2%	341,154
	February.....	116,608.....	38.0%	102,071.....	33.3%	76,447.....	24.9%	306,756
	March.....	112,605.....	35.9%	107,468.....	34.3%	81,093.....	25.9%	313,589
	April.....	90,384.....	31.7%	102,446.....	36.0%	80,460.....	28.2%	284,825
	May.....	100,331.....	32.6%	111,201.....	36.1%	84,661.....	27.5%	308,232
	June.....	120,116.....	36.0%	115,745.....	34.7%	84,992.....	25.5%	333,205
	July.....	153,749.....	39.5%	130,951.....	33.7%	90,752.....	23.3%	388,909
	August.....	150,083.....	38.9%	130,776.....	33.9%	91,062.....	23.6%	385,419
	September.....	131,567.....	37.3%	122,059.....	34.6%	86,160.....	24.4%	352,511
	October.....	107,997.....	33.7%	115,305.....	36.0%	84,396.....	26.4%	320,050
	November.....	102,453.....	34.4%	102,840.....	34.6%	79,625.....	26.8%	297,556
	December.....	121,078.....	37.6%	108,001.....	33.5%	80,095.....	24.8%	322,405
2020	January.....	124,414.....	38.4%	108,857.....	33.6%	77,426.....	23.9%	324,143
	February.....	111,931.....	37.1%	101,905.....	33.8%	75,650.....	25.1%	301,827
	March.....	104,006.....	35.0%	102,937.....	34.7%	77,565.....	26.1%	296,894
	April.....	97,465.....	36.3%	90,631.....	33.7%	69,591.....	25.9%	268,794
	May.....	105,412.....	37.5%	93,406.....	33.2%	71,220.....	25.3%	281,361
	June.....	131,242.....	40.2%	108,695.....	33.3%	75,211.....	23.0%	326,871
	July.....	166,891.....	43.2%	125,994.....	32.6%	81,276.....	21.0%	386,633
	August.....	158,821.....	42.3%	122,025.....	32.5%	82,582.....	22.0%	375,897
	September.....	127,584.....	38.8%	112,214.....	34.1%	77,505.....	23.6%	328,843
	October.....	105,537.....	34.4%	107,778.....	35.2%	81,861.....	26.7%	306,514
	November.....	99,385.....	35.0%	97,076.....	34.2%	75,851.....	26.7%	283,968

The values include sales to consumers reported by electric utilities and other energy service providers.  
Commercial sector includes public street and highway lighting and sales to public authorities.



Reducing electricity consumption in buildings is one of the categories, of measure to reduce greenhouse gas (GHG) emissions from buildings (Levine, *et. al*, 2007). By observing the energy consumption pattern of residential buildings, there are possible opportunities to reducing the contribution of residential buildings towards emissions. Levine *et. al.* estimate that “there is a global potential to reduce approximately 29% of the projected baseline emissions by 2020 cost-effectively in the residential and commercial sectors”. They argue that a wide array of “accessible and cost-effective technologies” such as passive solar design, high-efficiency lighting and appliances, highly efficient ventilation and cooling systems, solar water heaters, insulation materials and techniques as well as high-reflectivity building materials and multiple glazing (multiple sheets of glass in windows) can contribute to abate GHG emissions in buildings to a significant extent.

## **1.2 Human Comfort in the Winter Season**

When external factors are considered in the general case, the human body and the immediate environment envelope can be considered as a thermodynamic open system (Stoward, 1962 & Zotin, 1967). The body constitutes a diathermal sub-system within the open system which tries to maintain a steady temperature of 37°C (Chen, 1985). It tries to achieve this through a process known as homeostasis. Thermoregulation is one feature of homeostasis whereby core body temperature is regulated through vasomotion, sweating, and shivering thermogenesis (Psikuta, 2009). The ease with which the body achieves thermoregulation, with changes in physical factors such as the temperature gradient between the body and the environmental temperature, determines the levels of comfort. When human beings are in their homes, another diathermal sub-system envelope is created around the human body. The body

interacts directly with the immediate surroundings, heat transfer occurs, and the nature of this immediate surroundings directly affects the rate of thermoregulation and by extension, comfort.

### **1.3 Challenges of Heating Spaces in the Winter**

The temperature requirements for residential buildings change seasonally. ASHRAE recommends that indoor temperatures in the winter should be maintained between 20°C to 24°C (ASHRAE, 2020). Is there a model to be derived for air conditioning systems in modern buildings which will optimize and reduce power consumption by setting variable parameters such as number of vents, air exchange rate, air velocity, thermal properties of indoor equipment etc.

In the current study, by means of experimental and numerical analysis, building models for heating system will be investigated by examining the effects of altering the location of air vents, and the flowrate on thermal conditions in a control space. The goal is attaining the ASHRAE target temperature range for comfort, over prolonged periods with different compositions of the control volume. Observation of heat dissipation and preservation in the indoor thermal environment under different physical conditions in the control volume will be compared with Numerical CFD simulations performed using Simscale Flow Simulation.

## **2 Building Model**

### **2.1 Building Codes**

Construction and set up of buildings are guided by a combination of international, national, and local codes. The local codes are adopted from the International Code Council and modified for local area administrations. Local Administrations oversee the guidelines for the construction of residential buildings to establish minimum requirements for the safety of public use, health and general welfare while considering affordability, structural strength, means of egress facilities, stability, sanitation, light and ventilation, energy conservation and safety to life and property in general (Division of Building Safety, 2020)

In the state of Idaho for example, the Idaho Residential Code (which adopts with amendments the International Residential Code) makes provisions for the Residential codes for One- and Two-family dwellings.

### **2.2 Residential Building Codes**

State residential codes applies to the construction, use, occupancy etc. of one- and two-family dwellings. The code defines a residential building as “*any one or two-family dwelling or portion thereof, including townhouses, used or intended to be used for human habitation, for living, sleeping, cooking or eating purposes, or any combination thereof, or any accessory structure*” (Idaho Residential Code, 2020). These code specifications determine the selection of materials, which in turn also affect the thermal properties of building materials. The Idaho Residential Code provides guidelines for critical areas such as structural design, load under different external conditions.

## 2.3 Building Sample

For HVAC designs, the Air Conditioning Contractors of America (ACCA) Manuals provide a guide for the design of energy efficient cooling and heating setups for residential homes. Figure 2.1 shows the floor plan for a “Chicago House”, a theoretical house that meets the 2009 International Energy Conservation Code (IECC) energy efficient house. The house is modeled in the IECC Climate Zone 5 - CZ5 (see section 2.4), Chicago, Illinois.

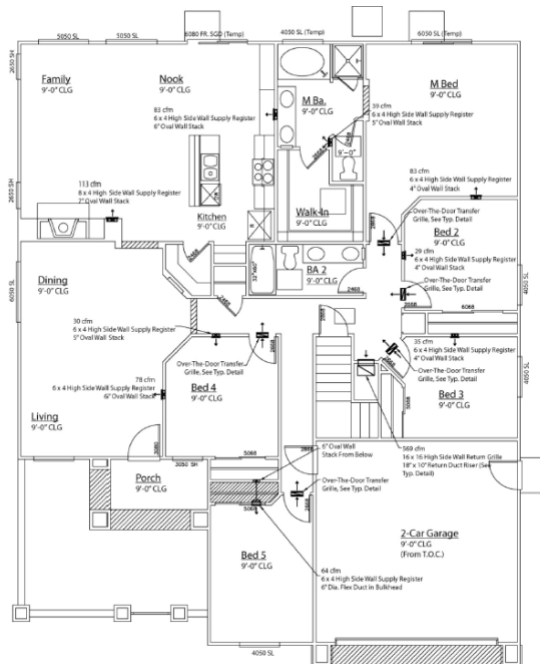


Figure 2.1 Chicago House, an energy efficient design used for testing ACCA standards (Burdick, 2011)

## 2.4 Standard External/Internal Conditions

The International Energy Conservation Code (IECC) regulates the minimum energy conservation requirements for modern buildings. The requirements for materials, design and setup of buildings are influenced by climate zones. The IECC manual (International Code Council, 2011) has set benchmarks for buildings depending on a ‘load’ which is calculated by considering some factors. The IECC residential code requirements use the concept of a building envelope in evaluating the

needed thermal resistance. The objective is to keep as much heat within the boundary as possible. Within the boundary, there are sub-systems, and the heat may cross by means gradients within the universal boundary. For purposes of design, the conditions outside this thermal

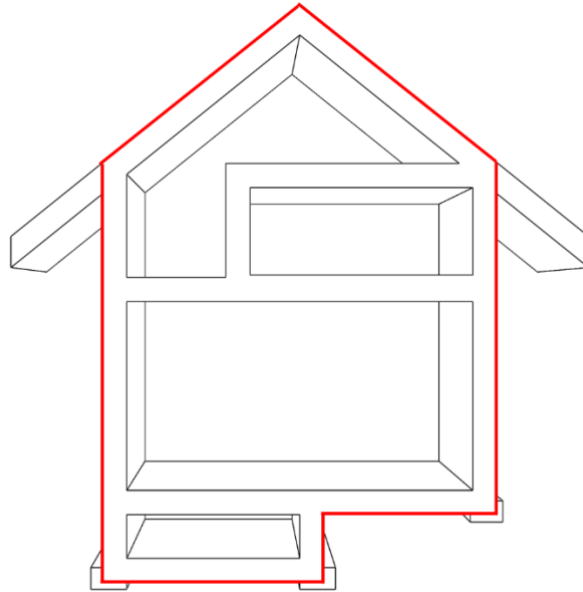


Figure 2.2 Concept of a universal thermal boundary. The objective of energy efficient buildings is to retain heat energy within this thermal boundary, energy may cross boundaries within sub-systems

boundary have been tabulated and standardized and are contained in the IECC manual for designers and engineers. The designs and analysis used by Burdick (2011) for the discussions and analysis of Chicago house are based on this manual. When the outside conditions are established based on the recommendations of the IECC manual, the designer must calculate the load requirement which then informs the choice of equipment and heat delivery system.

## **2.5 Building Heating Load Assessment**

Load calculation is the first step in ventilation design. In the current study, within the thermal envelope, an estimated heating load can be calculated based on certain design parameters. The heating load is that which is required to meet the inside design conditions, therefore it is the

measure of energy that a heat removal system needs to remove from a space to provide the desired level of comfort (Burdick, 2011, p. 3).

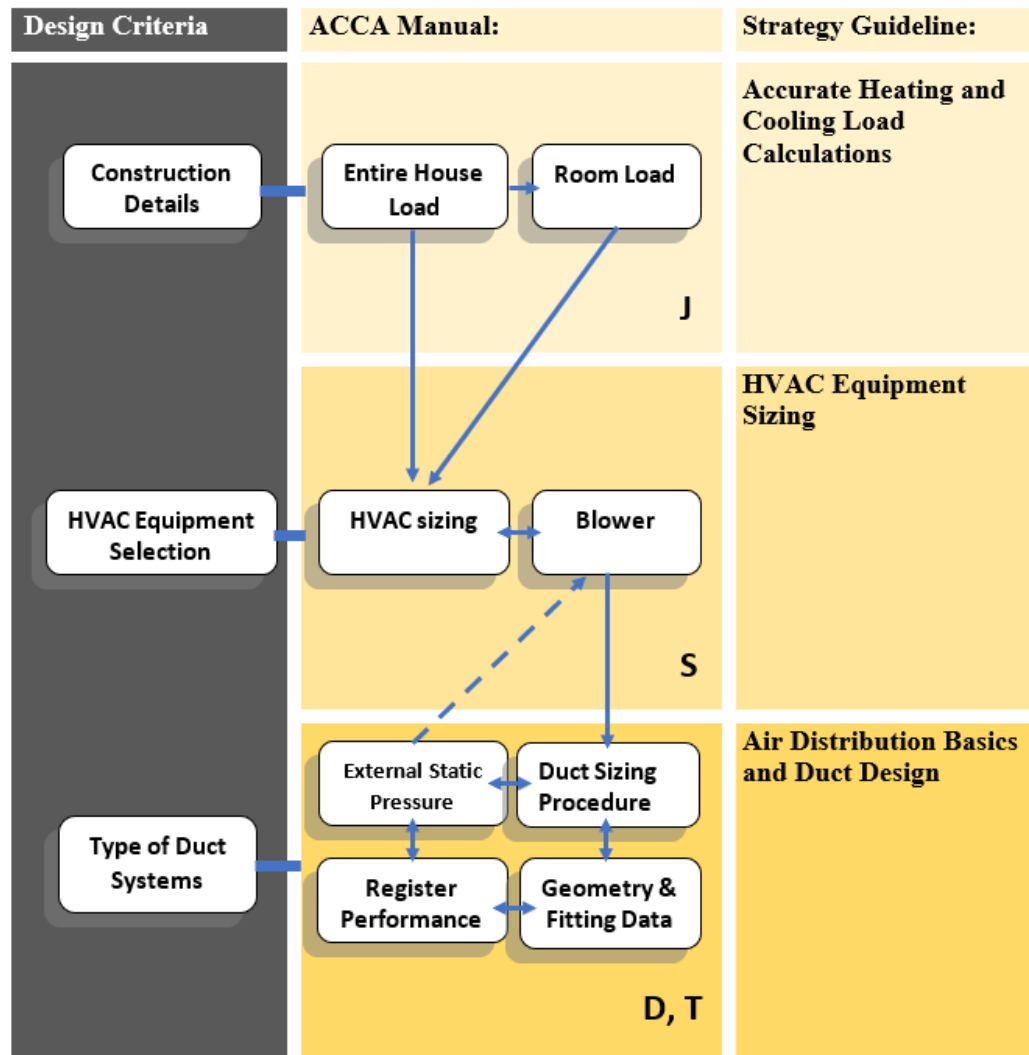


Figure 2.3 Steps in designing a building HVAC system

The Air Conditioning Contractors of America (ACCA) Manual J provides the detailed steps required to calculate the heating and cooling loads. The accurate heating and cooling loads are used to determine the right-size of equipment with ACCA Manual S Residential Equipment Selection, then to design the air distribution system and ductwork with ACCA

Manual T Air Distribution Basics for Residential and Small Commercial Buildings and ACCA Manual D Residential Duct System Procedure.

## **2.6 Forced Air Circulation Systems**

A forced air circulation system works by delivering heated air to a building by means of grills and air registers (American Council for Energy Efficient Economy, 2021). Air registers are usually placed at the ends of ducts. The heated air is derived by means of forced heat convection transfer of heat from a furnace to air. The form of energy used in powering the furnace is determined by ACCA manual S.

## **2.7 Building Thermal System**

The heat energy in the air circulated in a building is lost by convection and heat conduction through the building's walls. In a forced air circulation system, as the air is delivered into the building space, convective currents convey the heat around in the air column. Figure 2.4 shows the top profile of a column of air enclosed by insulated walls. There is an air inlet and outlet through which air flows in and out of the space. Say, that warm air is supplied into the enclosed space by means of a fan, the air in that space will be forced to flow over the surface of the walls thereby encouraging convective transfer of heat to the walls. Air is used to deliver warmth into the space, this warmth is useful for bringing thermal comfort especially during winter when the temperature gradient between the inside the house and outside is at its highest. Air velocity delivers the much-needed heat, but it also promotes loss of energy to the surroundings when a temperature gradient is established. Materials design and standards such as those described in the IECC manual aim to reduce the potential for this heat loss. Since, the engineer has control over the amount of energy that is added to the control space over a period, parameters such as the flow rate, size of vents, location of vents and number of

vents etc. can be modified for research as well as performance. However, it is important to understand how much of energy is lost to the walls and surrounding in each setup.

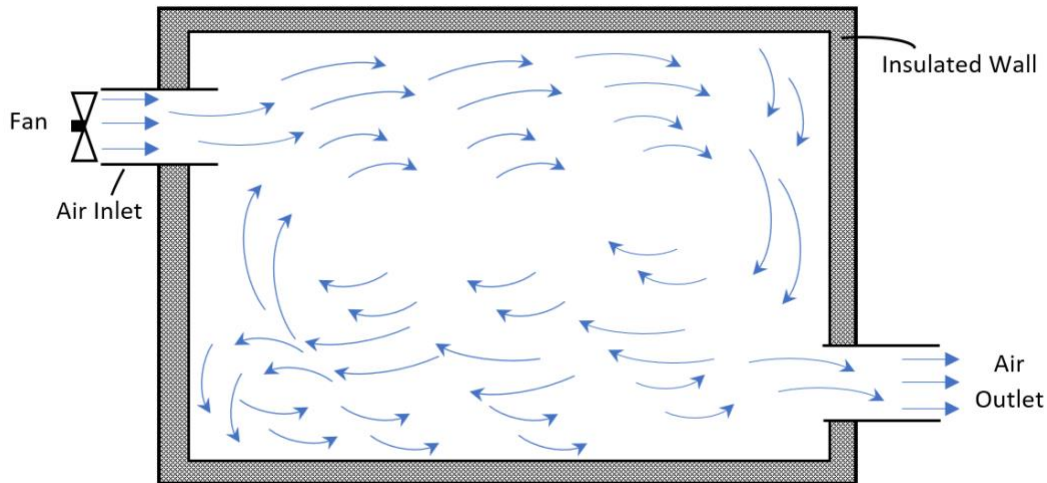


Figure 2.4 Air circulation in an insulated room

Convection heat transfer depends on the fluid properties dynamic viscosity  $\mu$ , thermal conductivity  $k$ , density  $\rho$ , specific heat  $cp$ , as well as the fluid velocity  $V$  (Çengel & Ghajar, 2020). The geometry of the surrounding walls, roughness of the solid surface, and fluid flow condition can also affect the heat transfer rates.

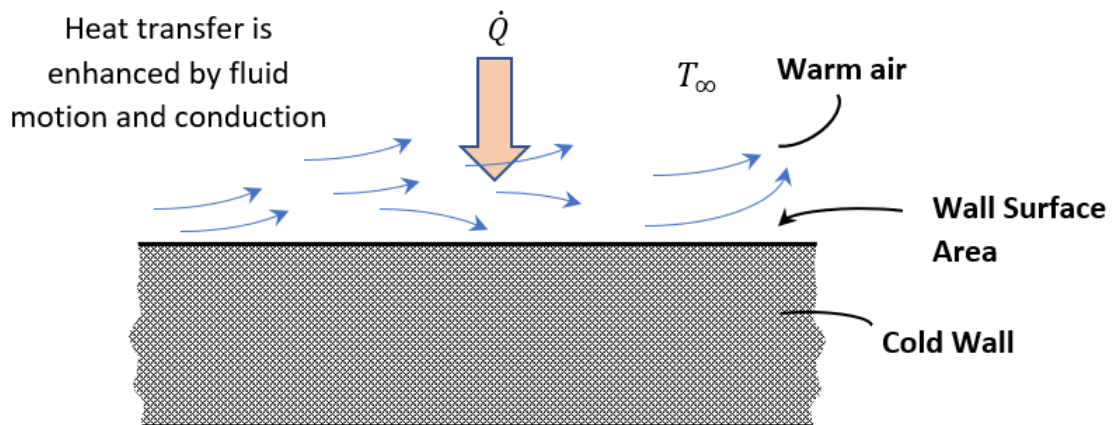


Figure 2.5 Forced Circulation promotes heat transfer

Newton's law of cooling is used in investigating the amount of heat transfer  $Q$



$$\dot{Q} = hA_w(T_w - T_\infty) \quad (1)$$

Where:

$h = \text{convection heat transfer coefficient} \left( \frac{W}{m^2 K} \right)$

$A_w = \text{measured wall surface area} (m^2)$

$T_w = \text{temperature of the wall} (^\circ C)$

$T_\infty = \text{temperature of the fluid at some point in the fluid} (^\circ C)$

In the region where the air column touches the wall (shown in figure 2.5), the fluid in motion has a region of zero velocity relative to the wall. At this region, the fluid sticks to the wall because of viscous properties of air and the wall. The layer of the fluid that sticks to the surface then slows the adjacent fluid layer because of viscous forces between the fluid layers, which slows the next layer, this phenomenon known as the no-slip condition is significant because a boundary layer can be developed (Cengel & Ghajar, 2020).

At the wall boundaries, on both sides of the wall where there is an interaction between the wall and the warm column of air and the cold winter air; it is important to observe how conduction takes place through the wall. Energy moves along a thermal gradient line; hence energy is lost from the warm air in the room to the surroundings.

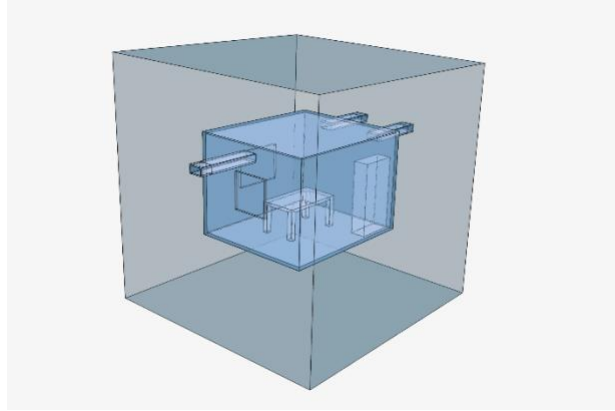


Figure 2.6 The outside wall of the building loses heat to surrounding air

Consider a column of cold winter air which contains a building. As shown in in figure 2.6 a column of air is contained on both sides of the insulated wall. The temperature gradient is created between the warm air and the cold air on the outside of the house.

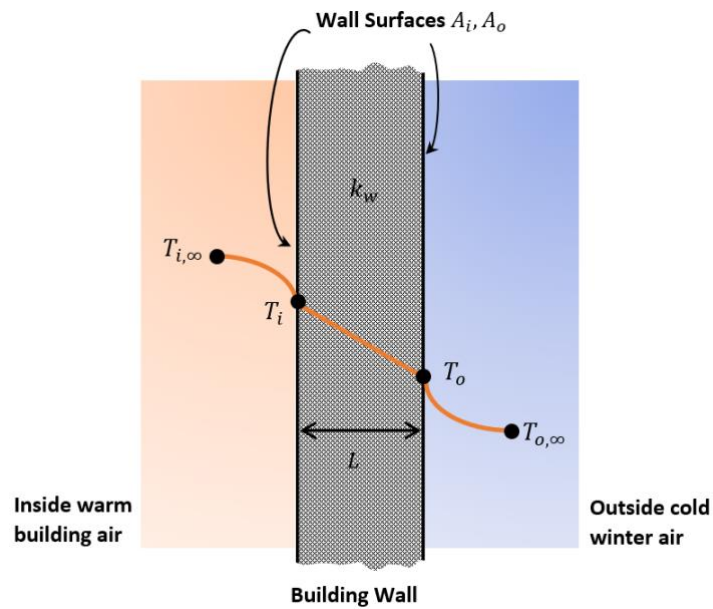


Figure 2.7 Heat conduction through the building's walls

From figure 2.7, the assumption can be made about the condition of the energy travelling through the building walls. For a steady state case, there is no change in the temperature

of the wall with time at any point. So, there is conservation of energy as heat is transferred, hence the rate of heat transfer through the building wall must be constant. If the wall thickness is taken to be  $L$ , the average thermal conductivity  $k_w$ , temperature on the inside and outside wall surfaces,  $T_i$  and  $T_o$  respectively and the surface area  $A$  then if the heat loss is one-dimensional steady heat conduction through the wall, then from theory, Fourier's law of heat conduction for the building wall can be expressed as

$$\dot{Q}_{wall} = k_w A \frac{T_i - T_o}{L} \quad (2)$$

Where  $\dot{Q}$  is the rate of heat conduction through the wall.

From Cengel & Ghajar (2020), where no bulk motion exists in a medium, like the movement of thermal energy through a wall, heat energy moves from the more energetic parts to adjacent less energetic solely by conduction. This movement of heat possesses direction as well as magnitude. A rectangular coordinate system is used describing the thermal conditions at any point medium. The equations which describe fluid flow and heat transfer can all hence be expressed in multiple dimensions. A point Temperature of interest  $T$  (figure 2.8) is described in 3 directions and by a time quantity (for transient state considerations). The

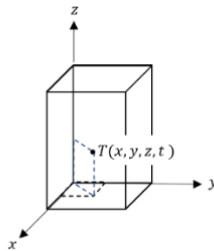


Figure 2.8 Rectangular Coordinate System: Fluid Flow and Heat Transfer  
Equations can be expressed in multiple dimensions

multidimensional heat transfer analysis for a building takes into consideration the heat loss or gain in the system by the 3 forms of heat transfer: conduction, convection, and radiation.

### **3 Methodology**

#### **3.1 SimScale Dashboard**

SimScale is an online platform where simulation can be performed by users by making use of as many as 96 core machines (Simscale, 2021a). The platform provides an all-in-one simulation platform for CFD, FEA and Thermal analysis applications. Users can create free community accounts where they can view the Community forum, public projects library, and work bench. The SimScale Workbench features a dashboard which can be accessed in the free account. The dashboard is personal landing page where personal projects can be managed, and tools can be accessed.

##### **3.1.1 Creating a New Simulation Project**

By clicking the ‘New Project’ button on the Dashboard, a new project can be started, the following fields are filled:

- a. the Project Title,
- b. Public/Private Project Toggle,
- c. Project description,
- d. Category
- e. Tags
- f. Advanced Settings (optional)

## Heat Flow through a Room

[Dashboard](#) > [Heat Flow through a Room](#) > [Edit](#)

The screenshot shows the 'Edit' page for a project titled 'Heat Flow through a Room'. The form includes a 'Project Title\*' field with the text 'Heat Flow through a Room', a 'Project Description\*' field with the text 'Test the heat flow through a 12x8x8ft room', a 'Choose a category' dropdown menu set to 'Validation', and a tag management section showing three tags: 'CONVECTIVE HEAT TRANSFER', 'COMFORT IN A ROOM', and 'HEAT TRANSFER', with a '3/12' indicator and an 'Add a tag' input. Below the tags is a 'Default unit system' dropdown menu set to 'Metric (Meter, Kilogram, Second, Celsius)'. At the bottom left, there is a 'Make private?' toggle switch and a link to 'Upgrade my plan'. A blue 'Update project' button is located at the bottom center.

Figure 3. 1 Project Creation Dialog (from <https://www.simscale.com>)

### 3.1.2 Importing the CAD Model

A CAD model is imported into the workbench by clicking on the geometry's icon on the dashboard. Users can import CAD files of different formats and orientations, for the current project, the CAD models were prepared using SolidWorks®.

### 3.1.3 Flow Volume Extraction

The region (control space) occupied by the fluid in the CAD model is then extracted from the CAD design. SimScale dashboard can detect the fluid encapsuled by boundaries by using the flow extraction tool. The feature has 3 different types of flow regions namely:

- a. Open Inner Region: This produces a fluid region which is an enclosed space with a limited number of openings to the outside. The extraction is performed by:

1. Selecting the boundary faces that lie between the external environment and the internal
  2. Selecting one internal seed face
  3. Running the extraction
- b. Closed Inner Region: This is defined as the enclosed space which does not have openings to the outside, but the space occupied by the fluid is void inside the model. The extraction for this feature is like the inner closed region case but without the boundary faces.
- c. Enclosure: This definition applies to predefined control volumes. It mostly used in external flow applications such the simulation of winds past a moving car.

The flow region contains the simulation domain for the simulation including the boundary layer and every subsystem listed in the system. After the flow has been extracted, a solid shape is produced, the dashboard recommends that the outer shell CAD design be deleted to reduce computational expense. The internal cavities and subsystems such as bodies, furniture etc. in the extracted volume region can be viewed by adjusting the render mode to translucent surfaces in the appearances tab.

#### **3.1.4 Topological Sets**

The subsystems in the extracted flow volume which have similar initial boundary conditions or properties can be grouped into sets. For example, all the windows or walls can be grouped into one topological set. Features in the CAD setup (within the flow volume) can be added to a single set by first highlighting all the subsystems and then clicking the “Create new set” button.

### 3.1.5 Creating the Simulation

The SimScale dashboard provides various simulation types. Table 3.1 shows a breakdown of the various simulations that be carried out on the dashboard. The simulations are grouped into Flow and Structural Categories. Users have the option of selecting one of the simulations from the categories.

Table 3.1 Simulation operations on the SimScale dashboard are grouped into 2 categories

<b>Flow</b>	<b>Structural</b>
Incompressible	Static
Incompressible (LBM)	Dynamic
Compressible	Heat Transfer
Convective Heat Transfer	Thermomechanical
Conjugate Heat Transfer	Frequency Analysis
Conjugate Heat Transfer v2.0	Harmonic
Multiphase	
Pedestrian Wind Comfort	

The choice and suitability of the type of simulation depends on the objectives of the experiment. There are similarities between some of the simulation types, like the Convective Heat transfer, Conjugate Heat Transfer and Conjugate Heat Transfer v2.0 options. The Conjugate Heat Transfer and Conjugate Heat Transfer v2.0 are ideal for cases where observation of the movement of heat between different mediums, like from solid to gas or liquid is to be carried out. The convective heat transfer option, however, is ideal for the investigation of heat transfer in

fluids by either natural convection or forced convection when flow motion is induced by external forces such as inlet pumps or fans. It also provides tools for modeling heat transfer by radiation.

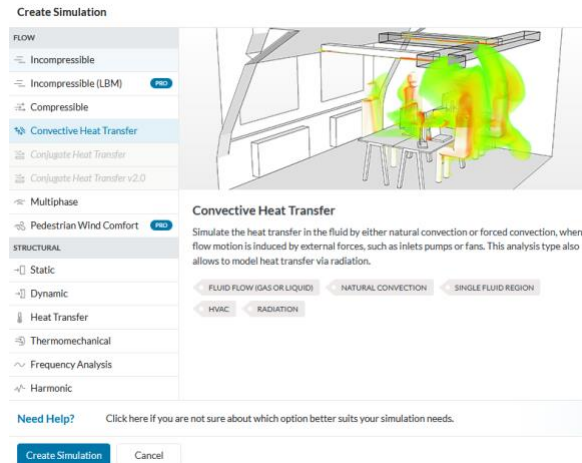


Figure 3.2 Convective Heat Transfer offers tools for simulating heat transfer in fluid media (from <https://www.simscale.com>)

### 3.1.6 Global Settings

After selecting the simulation type in the dialogue box, users can then “create simulation”. This brings up the dialogue box where the main simulation attributes can be set as shown in figure

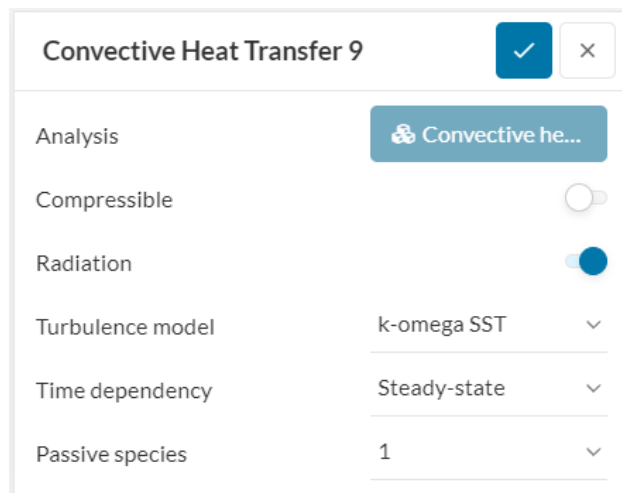


Figure 3.3 Convective Heat Transfer global conditions (from <https://www.simscale.com>)

3.3. Radiation heat transfer, compressibility, turbulence model, time dependency and passive species options can be set here.



#### a. Compressibility

In the Simscales® dashboard, the choice of a compressible or incompressible flow simulation is determined by the conditions of the fluid movement within the proposed simulation. Global compressible fluid flow conditions are ideal for fluid conditions where fluid density variations must be considered. Typically, it is recommended that compressible fluid flow analysis be employed where flow velocities exceed 30% of the speed of sound, approximately 100 m/s. (Simscales, 2021c). Where velocities are expected to be small (less than 100 m/s), incompressible fluid flow analysis is used, and density variations are ignored.

That is, divergence of flow velocity ( $u$ ) is zero (Simscales, 2021d).

$$\nabla \cdot u = 0 \tag{3}$$

#### b. Radiation

If the radiation button is toggled on, the Simscales simulator takes radiative form of heat transfer from surfaces into consideration. The heat energy from sunlight coming in through the windows makes this a desirable option for the current study.

#### c. Turbulence

The Simscales solver provides options on how to solve the turbulence equations at the inlets and accurately model the effects of turbulence. Models available include standard k-omega, baseline k-omega, k-omega SST etc. these models are ideal for different flow conditions. For this simulation the k-omega SST model was adopted. The k-omega SST (Shear Stress Transport) has to the ability to switch between two different models to “account for the transport of principal shear stress in adverse pressure gradient boundary layers” (Simscales, 2021b).

#### d. Time dependency

The simulation can be steady-state or transient. The steady state simulation on the SimScale platform produces the converged steady-state solution and less computationally expensive.

#### e. Passive Species

Passive Scalar source is a scalar quantity that can be used to model the propagation of species present in a fluid in low concentration (Simscale, 2021e). The species could be any component being transported by the fluid flow like smoke, oxygen bubble in water flow etc. The species quantity has to be small and not involved in the flow. Passive scalars can be used to also model the mean age of air of a fluid, which tests the freshness of air in a room. To set up the passive scalars, the global value is set to a small value like 1 and the initial value is set to 0. The turbulent Schmidt number which represents the ratio between the turbulent transport of momentum and turbulent transport of mass is set to a recommended value of 0.7 (Simscale, 2021f).

### **3.1.7 Thermal Comfort Assessment**

The dashboard provides a valuable tool, a thermal comfort function. Simscale's thermal comfort parameter outputs are based on two standards: ASHRAE 55 and ISO 7730 (Jenkins, 2020).

Simscale documentation provides background information on these standards and have been developed to specify a combination of indoor thermal environmental factors required to produce thermal environmental conditions that human occupants of a volume under observation will find comfortable (ASHRAE, 2020). The standards predict thermal comfort by assessing factors such as air temperature, thermal radiation, humidity, air speed, as well as personal factors such physical activity and clothing. The parameters used to gauge thermal comfort on the dashboard

are the Predicted Mean Vote (PMV) and Predicted Percentage of Dissatisfied (PPD) (Simscale, 2021g).

Table 3.2 Thermal Comfort input parameters (Simscale, 2021g)

Parameter	Unit	Standard Range	Simscale recommended
<b>Clothing Coefficient (<i>clo</i>)</b>	$1\ clo = 0.155$	ASHRAE-55: $[0, 1.5]\ clo$ ISO7730: $[0, 2]\ clo$	Summer: $0.5\ clo$ Winter: $1\ clo$
<b>Metabolic Rate (<i>met</i>):</b>	$1\ met$ $= 58.2\ W/m^2$	ASHARE-55: $[1, 2]\ met$ ISO 7730: $[0.8, 4]\ met$	$1\ met$ for passively sitting occupants $1.5\ met$ for actively sitting occupants
<b>Relative Humidity</b>		ASHARE-55: Accepted water vapor pressure: $[0 - 1910]\ Pa$ ISO 7730: Accepted water vapor pressure: $[0 - 2700]\ Pa$	

The results of a CFD evaluation are assessed based on table 3.3.

Table 3.3 Simscale's Thermal Comfort Assessment Output Interpretation (Buratti et al., 2015)

Thermal Sensation	Vote
<b>+3</b>	Hot
<b>+2</b>	Warm
<b>+1</b>	Slightly Warm
<b>0</b>	Neutral
<b>-1</b>	Slightly Cool
<b>-2</b>	Cool
<b>-3</b>	Cold

### 3.1.8 Simscale Meshing

The measurement of the heat transfer from the fluid to the walls of the room or control space in this study produces Partial differential Equations (PDE). The solution to these problems can be found by numerical methods however solving the problem conventionally can be tasking; the discretization of the equations and discretization of the domain provides a way out. The methods

of solving PDEs such as Finite Difference Method, Finite Volume Method and Finite element Method include the generation of a system of algebraic equations. Domain discretization provides a set of discrete cells which include points which ensure a continuous domain. The collection of these points connected in a network is known as a mesh (Simscale, 2021h). Meshes take geometric and topological forms and each cell within a mesh holds the solution of equations relevant to the local coordinates. Simscale's standard meshing algorithm known simply as Standard Mesher utilizes finite volume meshing (Simscale, 2021i). It creates a three-dimensional unstructured mesh with tetrahedral or hexahedral elements. The algorithm sets automatic values for the sizing to provide optimal performance. The refinement is recommended at 5 on a scale of 1 (very coarse) to 10 (very fine).

### **3.1.9 OpenFOAM®**

Simscale solver is based on OpenFOAM®, a free, open-source set of code used in performing CFD projects (OpenCFD, 2021). OpenFOAM has a wide range of capabilities especially features to solve complex fluid flow problems (Simscale, 2021j). With a collection of more than 250 applications and 100 software libraries, OpenFOAM executes CFD calculations either on single or multiple processors.

### 3.1.10 Setting up the simulation

The parameters to be set for the simulation are categorized as shown in Table

Table 3.3 Summary of Simulation Parameters

Section	Subsections	Parameters
<b>Model</b>		Turb Schmidt Number Diffusion Coeff Gravity
<b>Materials</b>		Add Materials like air, wood, glass etc.
<b>Initial Conditions</b>	Modified Pressure Gauge Velocity Temperature Turb. Kinetic Energy Specific Dissipation Rate Turb. Thermal Diffusivity Passive Scalar	Subdomains
<b>Boundary Conditions</b>		Add boundary conditions like Wall, Velocity, Pressure etc.
<b>Advanced Concepts</b>	Porous Media Power Sources Momentum Sources Passive Scalar Sources	Darcy-Forchheimer medium Fixed Coeff medium Etc.
<b>Numerics</b>		
<b>Simulation Control</b>		
<b>Result Control</b>	Forces and Moments Surface Data Probe Points Field Calculations	
<b>Mesh</b>	Refinements Meshing Logs Mesh Quality	

## 3.2 Experiment Setup

### 3.2.1 Baseline Control Volume

For this study, Bedroom 2 of the Chicago house which was covered in section 2.3 was adopted

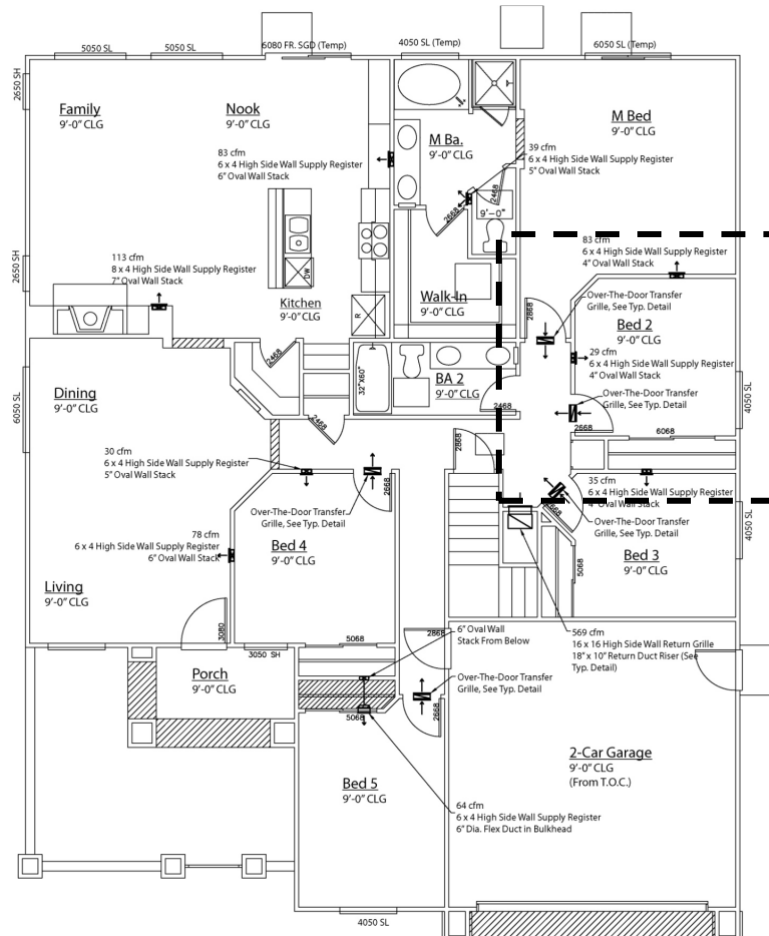


Figure 3.4 Chicago House Main Floor Plan, the box shows bedroom 2 highlighted, details are shown in figure 3.5

as the baseline model. The house is a multistorey building with the main floor plan shown in figure 3.4. Bedroom 2 floor plan and CAD designs are shown in figures 3.5 and 3.6 respectively. Specifications for the window, door, closet, and air vents are also shown in figure 3.5.

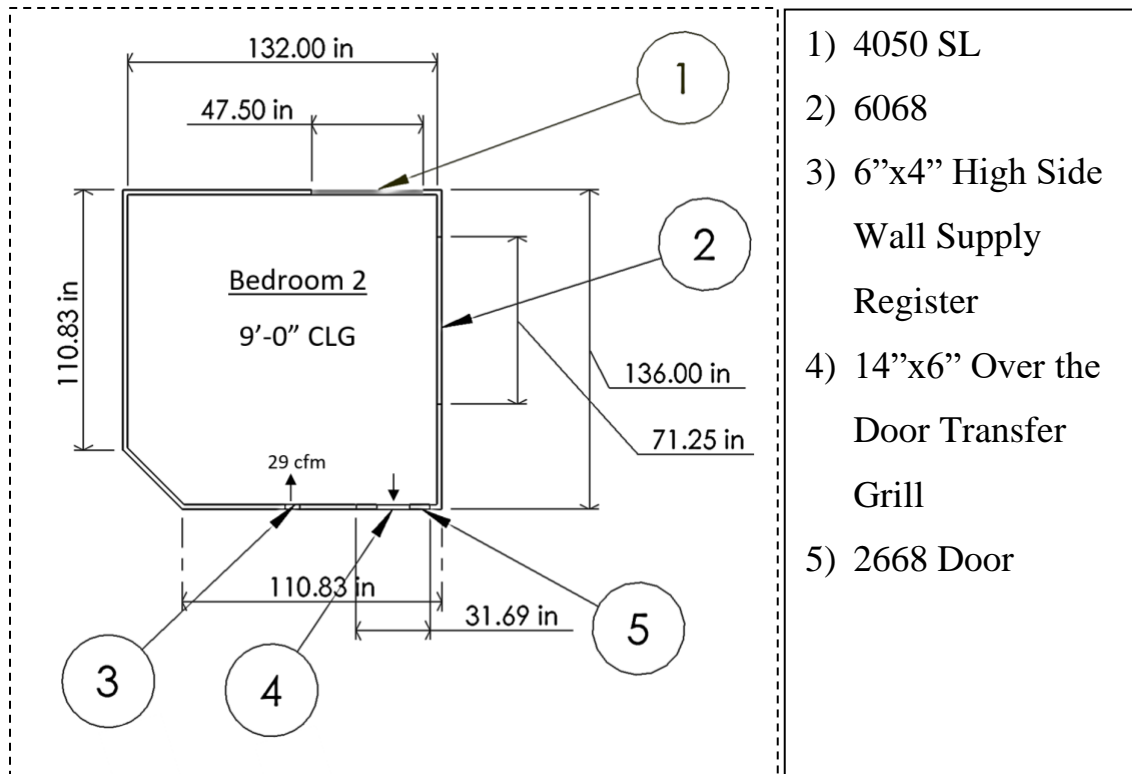


Figure 3.5 Bedroom 2 Chicago House Floor Plan

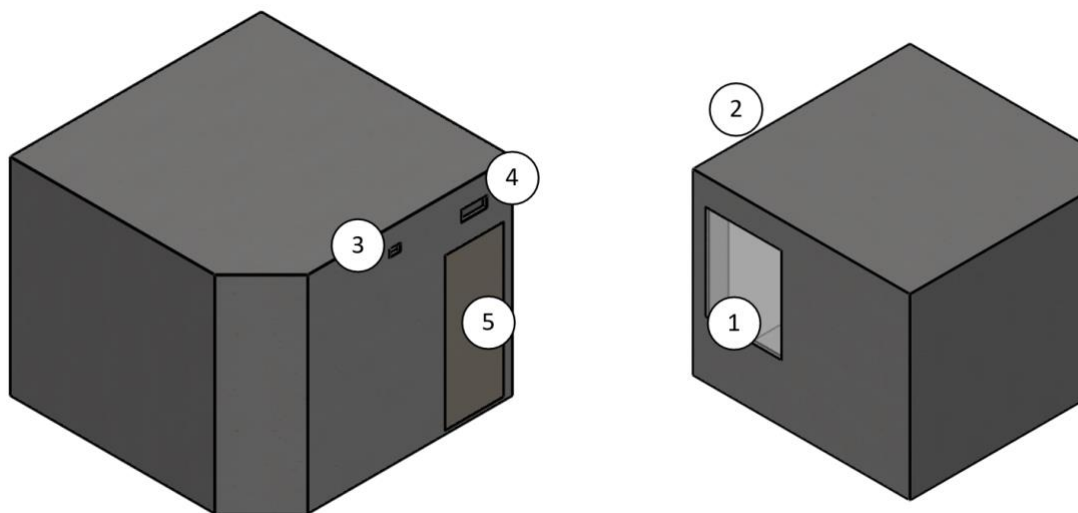


Figure 3.6 Bedroom 2 Front and Back views

The specifications for components 4050SL, 6068 and 2668 are listed in Appendix A, B and C respectively. With a ceiling height of 9 feet as shown in figure 3.5, this acts as the baseline for the experiment.

### 3.2.2 Materials

The control which consists of the surroundings, boundary and internal fluid have to be modelled accurately and as closely to the real case as possible. In this case, the surrounding air is the winter conditions in climate zone 5, where the baseline model house is located. The internal conditions are set by the baseline experiment conditions. The wall is a composite multilayer region which contains materials of different thermal properties which have to be evaluated. The internal and external fluid, SimScale provides a default approximation of the properties of air which engineers can use in running simulations which have air as the flow medium. Table 3.4 below shows the properties of air as listed in the SimScale documentation.

Table 3.4 SimScale Air Properties

Property	Value
Viscosity Model	Newtonian
Kinematic viscosity	$1.529 \times 10^{-5} \text{ m}^2/\text{s}$
Density	$1.196 \text{ kg}/\text{m}^3$
Thermal expansion coefficient	$3.43 \times 10^{-3} \text{ 1}/\text{k}$
T=Reference Temperature	273.1 K
Laminar Prantl Number	0.713
Turbulent Prandtl Number	0.85
Specific Heat	$1004 \text{ J}/\text{kgK}$



### 3.2.3 Baseline Parameters

The baseline parameters used for the design of the boundary conditions are derived from Burdick (2011) and are shown in table below.

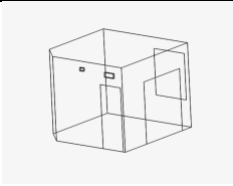
Table 3.5 Baseline Model Parameters

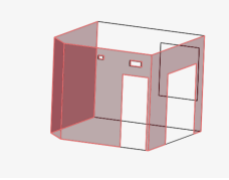
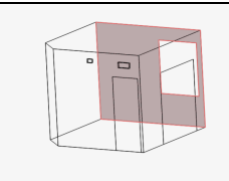
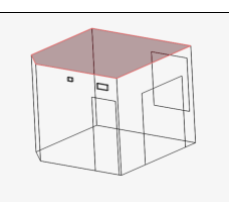
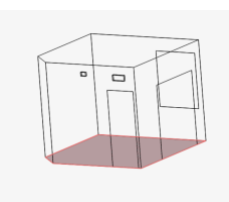
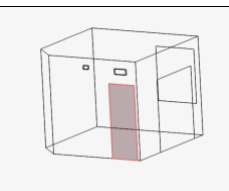
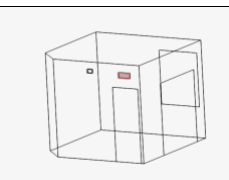
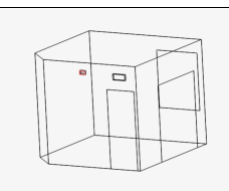
Condition	Parameters
Outdoor Temperature	$2F$
Indoor Temperature	$70F$
Wall Assembly	9' height, 2"x6" Framed walls, $R = 19$ , OSB Exterior sheathing, Brick Exterior, ½ inch interior drywall
Windows	$U = 0.35, SHGC = 0.5$
Inlet Flowrate	$29\text{ cfm}$

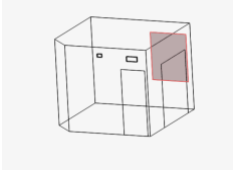
### 3.2.4 Boundary Conditions

Regions within the boundary of the control space were grouped into topological sets as shown in Table 3.6.

Table 3.6 Topological Sets

Topological sets	
Control Space	

Internal Walls	
External Wall	
Ceiling	
Floor	
Bedroom Door	
Outlet	
Inlet	

Window	
--------	--

These topological sets will have the same boundary conditions for all simulation runs, in some cases, more than one topology will have the same boundary conditions as will be shown in the coming sections.

#### **3.2.4.1 Adiabatic Wall Boundary condition**

Adiabatic boundary condition implies a zero-gradient condition between the cell values on both sides of the boundary surface (Oezcan, 2020). Due to the setup of the Chicago house as described in figure 3.4 the walls which make up the internal walls topological set, were set as adiabatic. This condition also affects the Ceiling, Floor and Bedroom Door topological sets.

Adiabatic Walls

✓

×

Boundary conditions	Wall	▼
(U) Velocity	No-slip	▼
Turbulence wall	Wall function	▼
Temperature type	Adiabatic	▼
Radiative behaviour	Opaque	▼
Emissivity	0.9	▼

Assigned Faces (17)

Clear list

Internal Wall

×

Ceiling

×

Floor

×

Closet

×

✕

Figure 3.7 SimScale Dashboard Setup

#### 3.2.4.2 External Wall Boundary condition

Externals walls interact with ambient conditions, in this case, a notable temperature gradient exists. To fully describe the nature of the interaction, the following parameters are set:

a. Ambient Temperature

The ambient temperature which is the temperature of the surrounding air is the value given in the Chicago House simulation which is winter conditions in climate zone 5. See table 3.5.

b. Heat Transfer Coefficient

The convective heat transfer  $h$  was evaluated by considering the rate of heat transfer from the vertical insulated wall by natural convection. Assuming steady operating conditions and air as an ideal gas as well as a local atmospheric pressure of 1 atm, the film temperature was derived as shown.

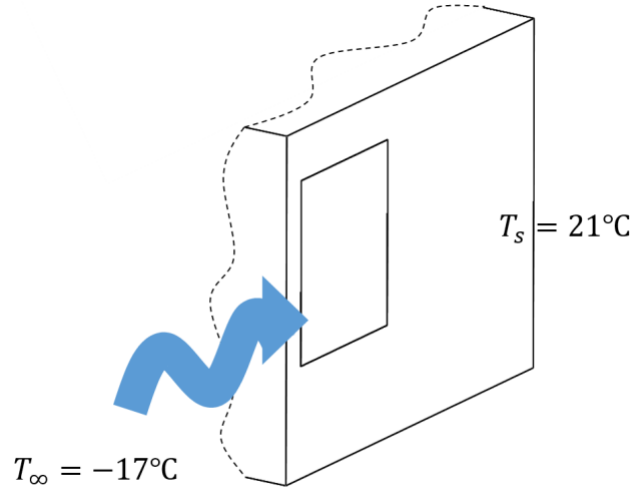


Figure 3.8 The air properties of wind blowing across the external wall

$$\text{The film temperature } T_f = \frac{T_s + T_\infty}{2} = \frac{21^\circ\text{C} + (-17^\circ\text{C})}{2} = 2^\circ\text{C} \quad (4)$$

$$\text{The volume expansion coefficient at film temperature } \beta = \frac{1}{T} \left( \frac{1}{K} \right) = \frac{1}{273+2} \left( \frac{1}{K} \right) = \frac{1}{275K} \quad (5)$$

From Cengel & Ghajar (2020) the properties of air at film temperature 2°C:

$$k \text{ thermal conductivity} \Rightarrow 0.2379 \frac{W}{m \cdot K}$$

$$Pr \text{ Prandtl number } 0.7360$$

$$\nu \text{ kinematic viscosity} \Rightarrow 1.3556 \times 10^{-5} \frac{m^2}{s}$$

$$L \text{ the characteristic length is the height of the wall} \Rightarrow 9 \text{ feet} = 2.7432m$$

$$g \text{ gravity} \Rightarrow 9.81 \frac{m}{s^2}$$

The Raleigh number for the characteristic length  $Ra_L \Rightarrow$

$$Ra_L = \frac{g\beta(T_s - T_\infty)L}{\nu^2} Pr \quad (6)$$

$$Ra_L = \frac{9.81 \frac{m}{s^2} \times \frac{1}{275K} \times [21-17]K \times 2.7432m}{\left(1.3556 \times 10^{-5} \frac{m^2}{s}\right)^2} \times 0.7360 \quad (7)$$

$$Ra_L = 1.4744 \times 10^{10}$$

Using the Nusselt number (Nu) formula  $\Rightarrow$

$$Nu = \left[ 0.825 + \frac{0.387 \times (1.4744 \times 10^{10})^{1/6}}{\left[ 1 + \left( \frac{0.492}{Pr} \right)^{9/16} \right]^{8/27}} \right]^2 \quad (8)$$

$$Nu = \left[ 0.825 + \frac{0.387 \times Ra_L^{1/6}}{\left[ 1 + \left( \frac{0.492}{0.7360} \right)^{9/16} \right]^{8/27}} \right]^2 \quad (9)$$

$$Nu = 286.7242$$

$$\text{Now, the convective heat transfer coefficient } h = \frac{kNu}{L} \text{ (Cengel \& Ghajar, 2020)} \quad (10)$$

$$h = \frac{0.2379 \frac{W}{m \cdot K}}{2.7432m} \times 286.7242 \quad (11)$$

$$h = 24.8657 \frac{W}{m^2 \cdot K} \quad (12)$$

### c. Contact conductance

The overall heat transfer coefficient for the multilayer wall. An examination of the construction of the wall for this setup shows that a pattern appears. This pattern is 17 inches long as shown in figure 3.9 and 3.25 inch deep. The depth is applied in thermal resistivity calculations.

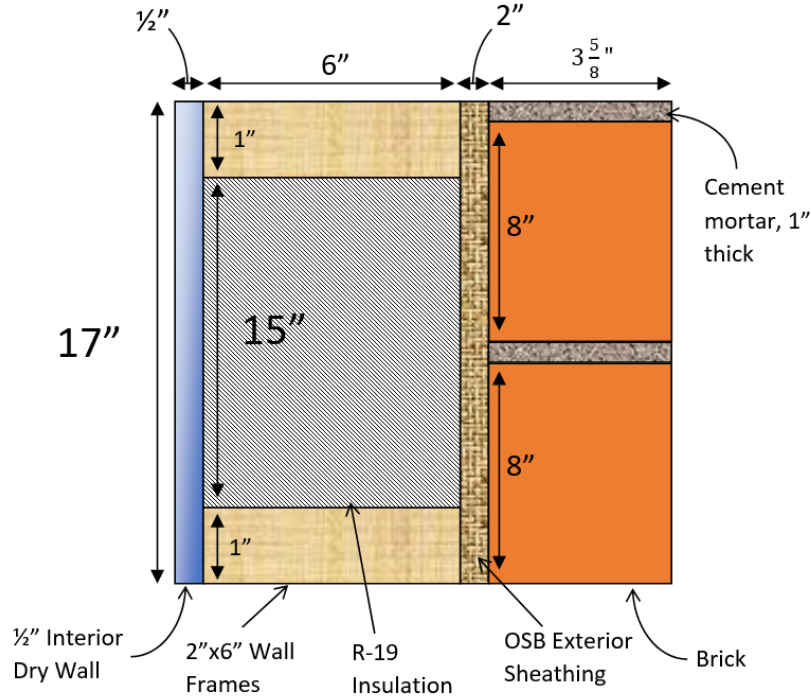


Figure 3.9 External Wall multilayer cross section

Figure 3.10 shows a cross-section of the layers through which heat will travel from the control space to the surroundings. Constant thermal conductivities are assumed for the case shown below

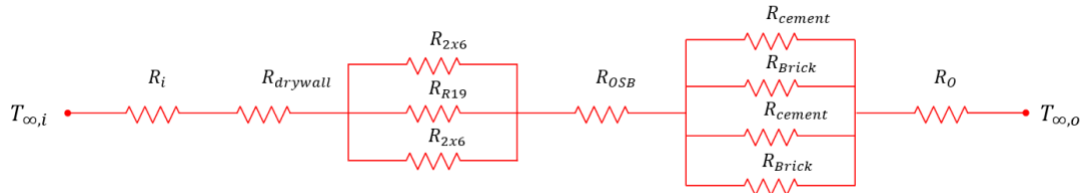


Figure 3.10 Thermal Resistance network for the external wall

If the multilayer regions within the cross section of the wall normal to the x-direction is assumed to be isothermal, the thermal resistance network for the portion of the wall shown can be represented by equation (13)

$$R_{total} = R_i + R_{drywall} + R_{sec1} + R_{OSB} + R_{sec2} + R_o \quad (13)$$

Where  $R_{sec1}$  and  $R_{sec2}$  are the combined resistances of the mid wall sections shown in parallel in figure 3.10. These combined are evaluated as follows:

$$\frac{1}{R_{sec1}} = \frac{1}{R_{2x6}} + \frac{1}{R_{R19}} + \frac{1}{R_{2x6}} \quad (14)$$

$$\frac{1}{R_{sec2}} = \frac{1}{R_{cement}} + \frac{1}{R_{Brick}} + \frac{1}{R_{cement}} + \frac{1}{R_{Brick}} \quad (15)$$

Evaluating the individual resistances

$$R_i = \frac{1}{h_i A_i} \quad (16)$$

Where  $A_i$  is the area of the inside wall (drywall) interacting with the ambient air in the building,  $h_i$  is the convective heat transfer coefficient between ambient air and the inside wall. The value of  $h_i$  is affected by the conditions of the air in the building as discussed in section 2.7. As shown in figure 2.5, the action of a blower or fan on the controlled air influences the rate of heat conducted through the wall. The value of  $h_i$  is therefore derived from considering the effect of forced convection on a plane vertical wall. With a characteristic length of 9 feet (height of the wall) the Reynolds number at the end of the airflow across the wall is

$$Re_L = \frac{VL}{\nu} \quad (17)$$

Where  $V$  is the airflow velocity measured in  $\frac{m}{s}$  and  $\nu$  is the kinematic viscosity. From table 3.5, the volumetric flowrate  $\Upsilon$  is given as  $29 \frac{ft^3}{m}$  and duct outlet of 6 inches by 4 inches. The airflow velocity acting along the wall can then be computed as

$$V = \frac{\Upsilon}{A} \quad (18)$$



$$\Upsilon = 29 \frac{ft^3}{m} = 29 \times \frac{1}{2119} \frac{m^3}{s} = 0.01369 \frac{m^3}{s} \quad (19)$$

The area of the outlet duct

$$A = 6in \times 4in = 0.1524m \times 0.1016m = 0.0155m^2$$

With the values of the volumetric flow rate and duct output area known, the velocity is then computed by using equation (18)

$$V = \frac{0.01369 \frac{m^3}{s}}{0.0155m^2} = 0.8841 m/s \quad (20)$$

Taking the surface temperature of the inside wall to be the film temperature derived in equation (4), the film temperature for the air inside the building is evaluated as the average between the ambient air temperature, given in table 3.5 as 70°F (approx. 21°C) and the wall temperature.

$$T_f = \frac{T_s + T_\infty}{2} = \frac{2^\circ C + 21^\circ C}{2} = 11.5^\circ C \quad (21)$$

Properties of air at 1 atm and 11.5°C (Cengel & Ghajar, 2020).

$$k \text{ thermal conductivity} \Rightarrow 0.0245 \frac{W}{m \cdot K}$$

$$Pr \text{ Prandtl number } 0.7332$$

$$\nu \text{ kinematic viscosity} \Rightarrow 1.4392 \times 10^{-5} \frac{m^2}{s}$$

$$L \text{ the characteristic length is the height of the wall} \Rightarrow 9 \text{ feet} = 2.7432m$$

Therefore, the Reynolds number for the characteristic length

$$Re_L = \frac{VL}{\nu} = \frac{0.8841 m/s \times 2.7432m}{1.4392 \times 10^{-5} \frac{m^2}{s}} = 1.6851 \times 10^{-5} \quad (22)$$

The value is less than the critical Reynolds number for flow over a flat surface  $5 \times 10^5$  (Cengel & Ghajar, 2020), therefore the flow is still laminar at this length. The formula for evaluating Nusselt number for laminar flow over flat surfaces is used to find the value of  $h_i$ .

$$Nu = \frac{h_i L}{k} = 0.664 Re_L^{0.5} Pr^{\frac{1}{3}} \quad (23)$$

$$Nu = 0.664 \times (1.6851 \times 10^{-5})^{0.5} \times (0.7332)^{\frac{1}{3}} \quad (24)$$

$$Nu = 245.8 \quad (25)$$

$$h_i = \frac{Nuk}{L} = \frac{245.8 \times 0.0245 \frac{W}{m \cdot K}}{2.7432 m} \quad (26)$$

$$h_i = 2.1952 W/m^2 K \quad (27)$$

Equation can now be evaluated to find the thermal resistance at the inside wall.

$$R_i = \frac{1}{h_i A_i} \quad (28)$$

$$A_i = 17 in \times 3.25 in = 0.4318 m \times 0.08255 m$$

$$R_i = \frac{1}{2.1952 W/m^2 K \times 0.4318 m \times 0.08255 m} = \frac{1}{0.0782 W} = 12.78 \frac{K}{W} \quad (29)$$

For  $R_{drywall}$

$$R_{drywall} = \frac{L}{kA} \quad (30)$$

From figure 3.9, the thickness of the drywall is  $0.5 in$  ( $0.0127 m$ ), and the thermal conductivity  $k$  is  $0.17 \frac{W}{m \cdot K}$  (Engineering Toolbox, 2003), therefore

$$R_{drywall} = \frac{L}{kA} = \frac{0.0127m}{0.17 \frac{W}{m \cdot K} \times 0.4318m \times 0.08255m} = 2.0958 \frac{K}{W} \quad (31)$$

The resistance  $R_{2 \times 6}$

From figure 3.9, the thickness of the 2x6 frame is *6in* (0.1524m), the thermal conductivity  $k$  of Douglas-fir 12% ovendry wood is  $0.12 \frac{W}{m \cdot K}$  (TenWolde et al., 1988), it only covers an area with length *1inch* (0.0254m) and depth of *3.25 inches* (0.08255m), therefore

$$R_{2 \times 6} = \frac{L}{kA} = \frac{0.1524m}{0.12 \frac{W}{m \cdot K} \times 0.0254m \times 0.08255m} = 605.694 \frac{K}{W} \quad (32)$$

The resistance  $R_{R19}$

From figure 3.9, the thickness of the R19 insulation is *6in* (0.1524m), the thermal conductivity  $k$  is  $0.5466 \frac{W}{m \cdot K}$ , it only covers an area with length *15 inches* (0.381m) and depth of *3.25 inches* (0.08255m), therefore

$$R_{R19} = \frac{L}{kA} = \frac{0.1524m}{0.5466 \frac{W}{m \cdot K} \times 0.381m \times 0.08255m} = 8.865 \frac{K}{W} \quad (33)$$

The resistance  $R_{OSB}$

From figure 3.9, the thickness of the board is *2in* (0.0508m), the thermal conductivity  $k$  is  $0.118 \frac{W}{m \cdot K}$  (Igaz et.al, 2017), it only covers an area with length *17inch* (0.4318m) and depth of *3.25 inches* (0.08255m), therefore

$$R_{OSB} = \frac{L}{kA} = \frac{0.1524m}{0.118 \frac{W}{m \cdot K} \times 0.4318m \times 0.08255m} = 12.078 \frac{K}{W} \quad (34)$$

The resistance  $R_{cement}$

From figure 3.9, the thickness of the cement mortar is  $3.65in$  ( $0.092075m$ ), the thermal conductivity  $k$  is  $0.173 \frac{W}{m \cdot K}$  (Engineering Toolbox, 2003), it only covers an area with length  $1inch$  ( $0.0254m$ ) and depth of  $3.25 inches$  ( $0.08255m$ ), therefore

$$R_{cement} = \frac{L}{kA} = \frac{0.092075m}{0.173 \frac{W}{m \cdot K} \times 0.4318m \times 0.08255m} = 25.283 \frac{K}{W} \quad (35)$$

The resistance  $R_{Brick}$

From figure 3.9, the thickness of the brick is  $3.65in$  ( $0.092075m$ ), the thermal conductivity  $k$  is  $0.47 \frac{W}{m \cdot K}$  (Engineering Toolbox, 2003), it only covers an area with length  $8inch$  ( $0.2032m$ ) and depth of  $3.25 inches$  ( $0.08255m$ ), therefore

$$R_{Brick} = \frac{L}{kA} = \frac{0.092075m}{0.47 \frac{W}{m \cdot K} \times 0.2032m \times 0.08255m} = 11.679 \frac{K}{W} \quad (36)$$

The resistance  $R_o$

$$R_o = \frac{1}{h_o A_o} \quad (37)$$

$$A_o = 17in \times 3.25in = 0.4318m \times 0.08255m \quad (38)$$

From equation (12)  $h_o = 24.8657 \frac{W}{m^2 \cdot K}$

$$R_o = \frac{1}{24.8657 \frac{W}{m^2 \cdot K} \times 0.4318m \times 0.08255m} = 1.128 \frac{K}{W} \quad (39)$$

From equation (14), the value for  $R_{sec1}$

$$\frac{1}{R_{sec1}} = \frac{1}{605.694 \frac{K}{W}} + \frac{1}{8.865 \frac{K}{W}} + \frac{1}{605.694 \frac{K}{W}} \quad (40)$$

$$\frac{1}{R_{sec1}} = \frac{1}{0.1161} \frac{W}{K} \quad (41)$$

$$R_{sec1} = 8.6128 \frac{K}{W} \quad (42)$$

From equation (15), the value for  $R_{sec2}$

$$\frac{1}{R_{sec2}} = \frac{1}{25.283 \frac{K}{W}} + \frac{1}{11.679 \frac{K}{W}} + \frac{1}{25.283 \frac{K}{W}} + \frac{1}{11.679 \frac{K}{W}} \quad (43)$$

$$\frac{1}{R_{sec2}} = \frac{1}{0.2504} \frac{W}{K} \quad (44)$$

$$R_{sec2} = 3.994 \frac{K}{W} \quad (45)$$

Equation (13), the total resistance is evaluated

$$R_{total} = R_i + R_{drywall} + R_{sec1} + R_{OSB} + R_{sec2} + R_o \quad (46)$$

$$R_{total} = 12.78 \frac{K}{W} + 2.0958 \frac{K}{W} + 8.6128 \frac{K}{W} + 12.078 \frac{K}{W} + 3.994 \frac{K}{W} + 1.128 \frac{K}{W} \quad (47)$$

$$R_{total} = 40.689 \frac{K}{W} \quad (48)$$

The total resistance for the wall under consideration  $R_{wall}$

$$R_{wall} = R_{total} \times Wall \text{ Area} \quad (49)$$

$$R_{wall} = 40.689 \frac{K}{W} \times 0.4318m \times 0.08255m \quad (50)$$

$$R_{wall} = 1.45 \frac{m^2 K}{W} \quad (51)$$

The overall conductance  $U$

$$U = \frac{1}{R_{wall}} = \frac{1}{1.45 \frac{m^2 K}{W}} = 0.69 \frac{W}{m^2 K} \quad (52)$$

d. Initial Boundary Temperature

The film temperature of 2°C described in the previous section was used as the initial boundary temperature for the internal face of the wall.

e. Wall Radiative Behavior

The emissivity is set 0.9 for simplicity and to simulate close to radiation from an ideal black surface.

## 4 Results and Discussions

### 4.1 Air Vent Location Performance

The temperature distributions for the different models are shown in figure 4.1. Cutting planes were

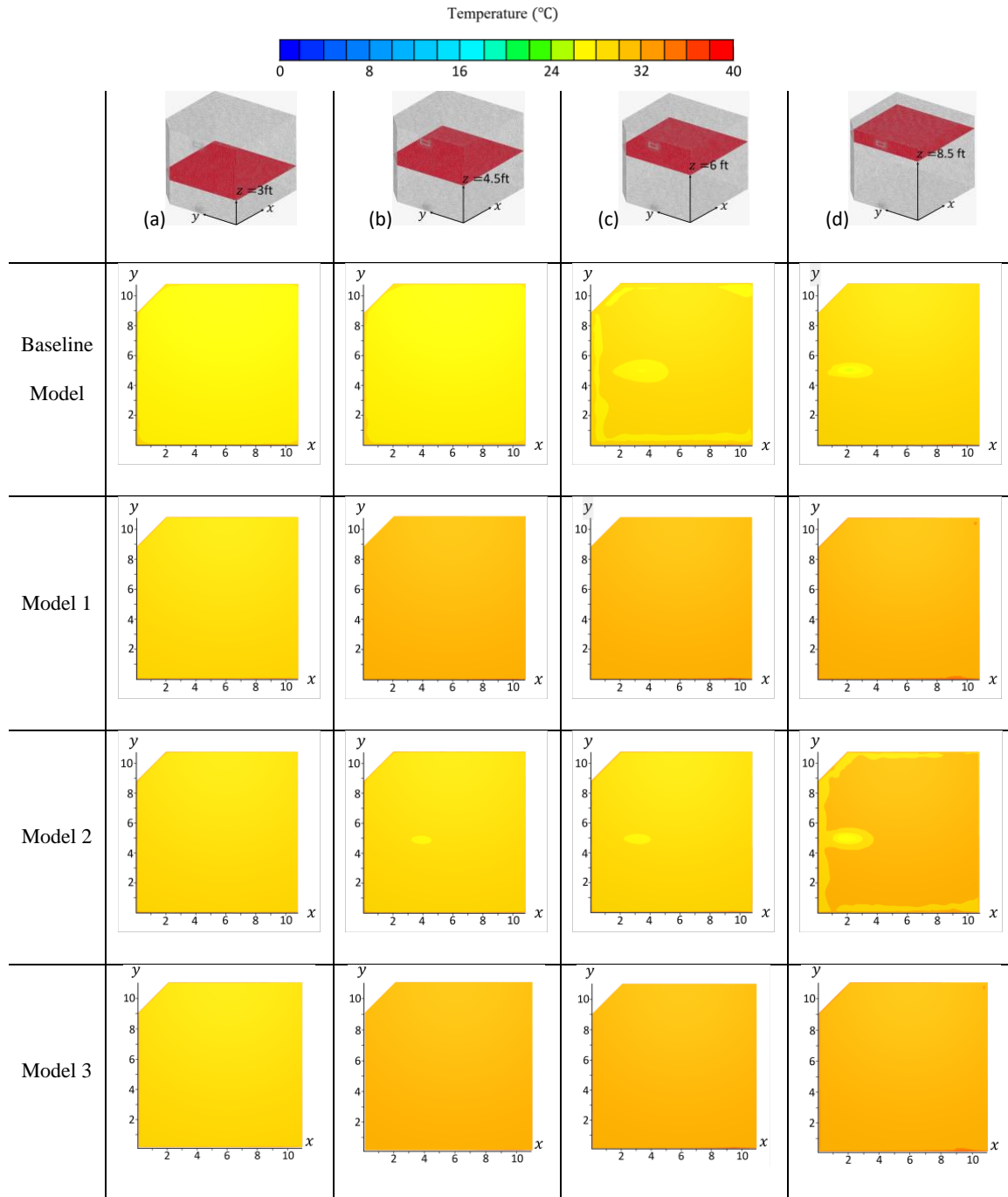


Figure 4.1 Top view temperature distribution profile for the various models at (a) 3ft, (b) 4.5ft, (c) 6ft and (d) 8.5ft above the floor. (Length measurements in the profiles are in feet)

set at 3, 4.5, 6 and 8.5 feet above the ground. In the baseline model, at elevations of 3 and 4.5 feet

above floor level, there is a constant temperature distribution of approximately 26°C; note that this temperature is above the air supply temperature of 21°C. At 6 feet above the floor in the baseline model, the temperature of the column is roughly 30°C and slightly higher than the section of air beneath. Figure 4.2 shows the side profiles of the temperature distributions and highlights this separation of air sections. The 26°C air column is the predominant air section, above this is the 30°C air section and then a thin film of air section at the top of the profile (Figure 4.2 baseline model(c)) which is not captured in the 8.5 feet cutting plane for the baseline model in figure 4.1. This points to the possibility of a film of air of less than 6 inches forming at the top of the room. In summary, the baseline model has at least 2 observable columns of air and a film close to ceiling boundary, the temperature variation in the model is approximately 4°C from top to bottom. Model 1 in contrast to the baseline model has at 4 different palpable air temperatures. The cutting planes for the top view elevations in figure 4.1 show a uniform distribution of temperature across all 4 registered elevations. From the color scheme, it can be observed that the temperature variation is as high as 10°C. The lowest air section is at about 26°C and the highest section is at about 36°C. There is a section which starts at about 1 foot and extends to 4 feet above the ground, then there is a middle section starting at about 4 feet above the ground and extending for another 4.5 feet. A human occupant in the room may experience different heat sensations at small elevation changes. The changes in temperature are also shown in the top view cutting planes in figure 4.1. However, it is observable that despite the presence of these different air sections, the temperature distributions at the cutting planes are relatively constant and evenly spread. In model 2, from figure 4.1 (d) column, a slight increase in temperature is at the 8.5 feet cutting plane. The side projection reveals that 2 clear air sections are present. An air film, not dissimilar from the one noticed in the baseline



model is also beginning to form in model 2. Temperature range in this model is approximately 2°C.

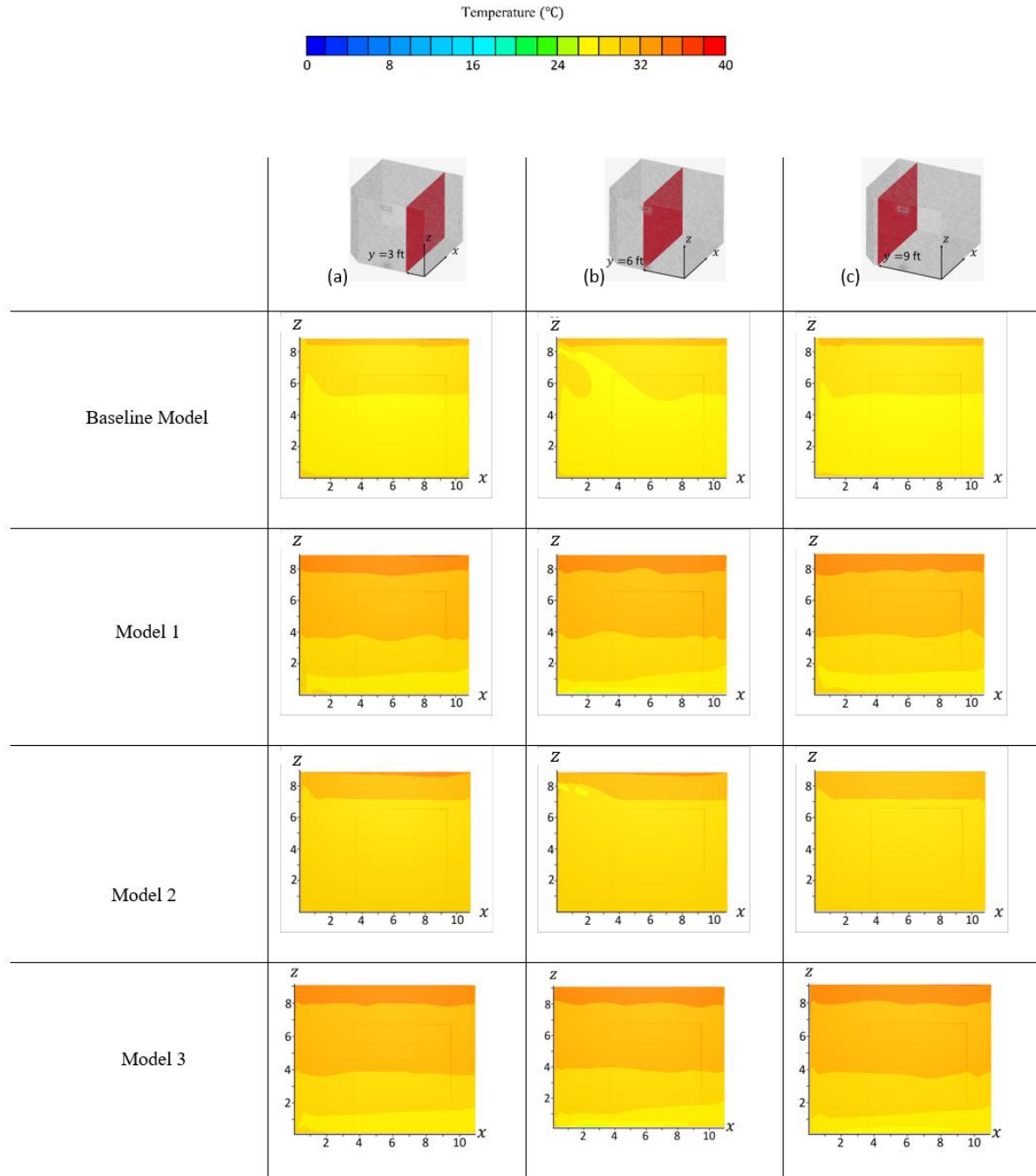


Figure 4.2 Side view temperature distribution profile for the various models at (a) 3ft, (b) 6ft and (c) 9ft from the side wall. (Length measurements in the profiles are in feet)

Model 3 is like Model 1, both models have the inlet vents at a lower register. Model 3 also has multiple air sections with temperature profile rising from the floor to the ceiling. The highest Temperature is also not captured at 8.5 feet above the ground.

#### 4.2 Inlet Air Velocity Performance

Figure 4.3 shows the air velocity distribution (column b) in the models. The velocity distribution is juxtaposed with the temperature distribution to highlight how the velocity relates with temperature distribution and at the inlet. From the color scheme, the velocity at the inlet is  $\approx 0.8 \text{ m/s}$  at the inlet. A similar value was computed numerically in equation (20) ( $V = 0.8841 \text{ m/s}$ ) for the velocity at the inlet. The velocity spread in the most areas of the room is below  $0.16 \text{ m/s}$ , this is way below the upper limit of ASHRAE standards for occupied zones (ASHRAE, 2017). The wake of the velocity spread for all 4 models is also within the 2 feet line which meets ACCA “occupied zone” requirements (Burdick, 2011).

Also, Models 1 and 3 (represented in figure 4.3 as 2 and 4 respectively) have similar setups with both models having inlet ducts and bottom registers. Their velocity profiles also show similar patterns. The disparity between the air outlet vent locations does not affect the velocity profiles of Model 1 and Model 3. There is however some variation in how parallel the inlet duct velocities are, Model 3 shows a velocity profile which is almost parallel to the room floor. The location of the outlet air ducts for models 1 and 3 differ and this may be a contributing factor for this difference. The wake of the warm air entering model 3 is also in line with the outlet vent, the pressure differential created by the  $0 \text{ Pa}$  outlet located vertical above keeps the velocity profile in line. This cyclical motion between the inlet and outlet can be observed in the baseline model and model 2 as well. The baseline model and model 2 (1 and 3 in figure 4.3) have similar vents but have outlet ducts in different locations. So, the cyclic motion triggers a ‘mixing’ action between

the air already in the room and the fresh jet of warm air entering the room.

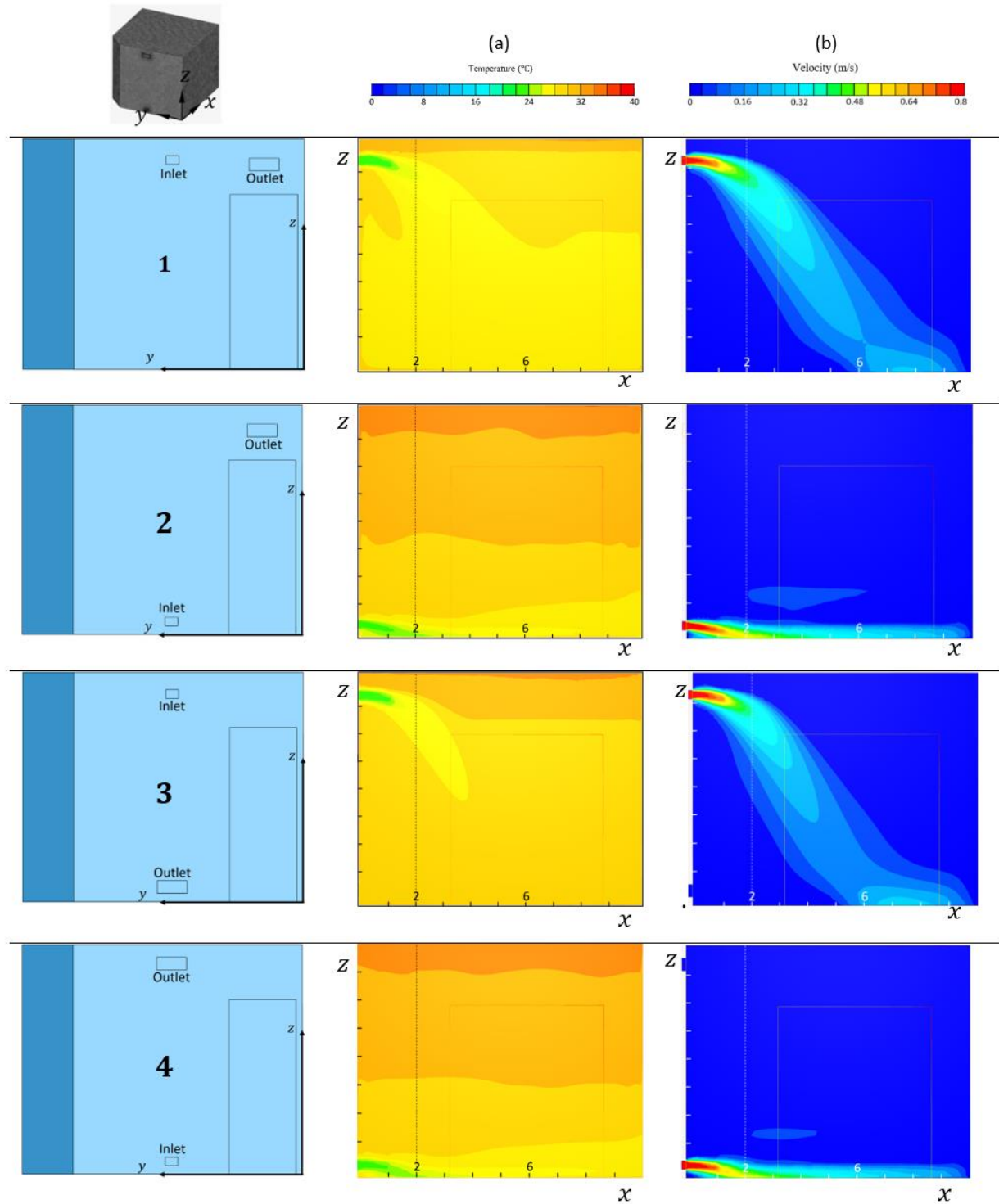


Figure 4.3 Inlet Performance for (1) Baseline Model (2) Model 1 (3) Model 2 and (4) Model 3. The columns (a) & (b) show the Temperature and Velocity side view profiles respectively. (Length measurements in the profiles are in feet)

Both inlet vents are elevated and therefore both also experience gravity leading them both to have a ‘waterfall’ effect.

### 4.3 Air Flow Rate Performance

In figures 4.4, 4.5, 4.6, and 4.7, the air flow rates in the baseline model, model 1, model 2, and model 3 respectively are manipulated and recorded. The baseline volumetric flow rate from Chicago house, bedroom 2 ( $29 \text{ ft}^3/\text{m}$  or  $0.14 \text{ m}^3/\text{s}$ ) was increased by 20% - 100% in steps of 20 and the simulations were restarted. The temperature distribution profiles were then compared. All 4 models show a gradual decline of heat retention. The temperature distribution is still predominantly above the air supply temperature. A higher volumetric rate means a greater amount of warm air will be supplied to the same volume in the same time frame and this creates a bigger pressure difference between the conditions inside the control space and the surroundings. This explanation is confirmed by reducing the flow rate. In figure 4.8 the flow rate was decreased by 20% and run again for all 4 models. In these cases, more heat is stored in the room over the same amount of time. The amount of heat lost through the external wall also reduces, because as highlighted in section 2.7, forced convection is heightened by increased air velocity. Slower supply of air reduces the rate of heat conduction through walls but also takes longer to adequately warm up spaces.

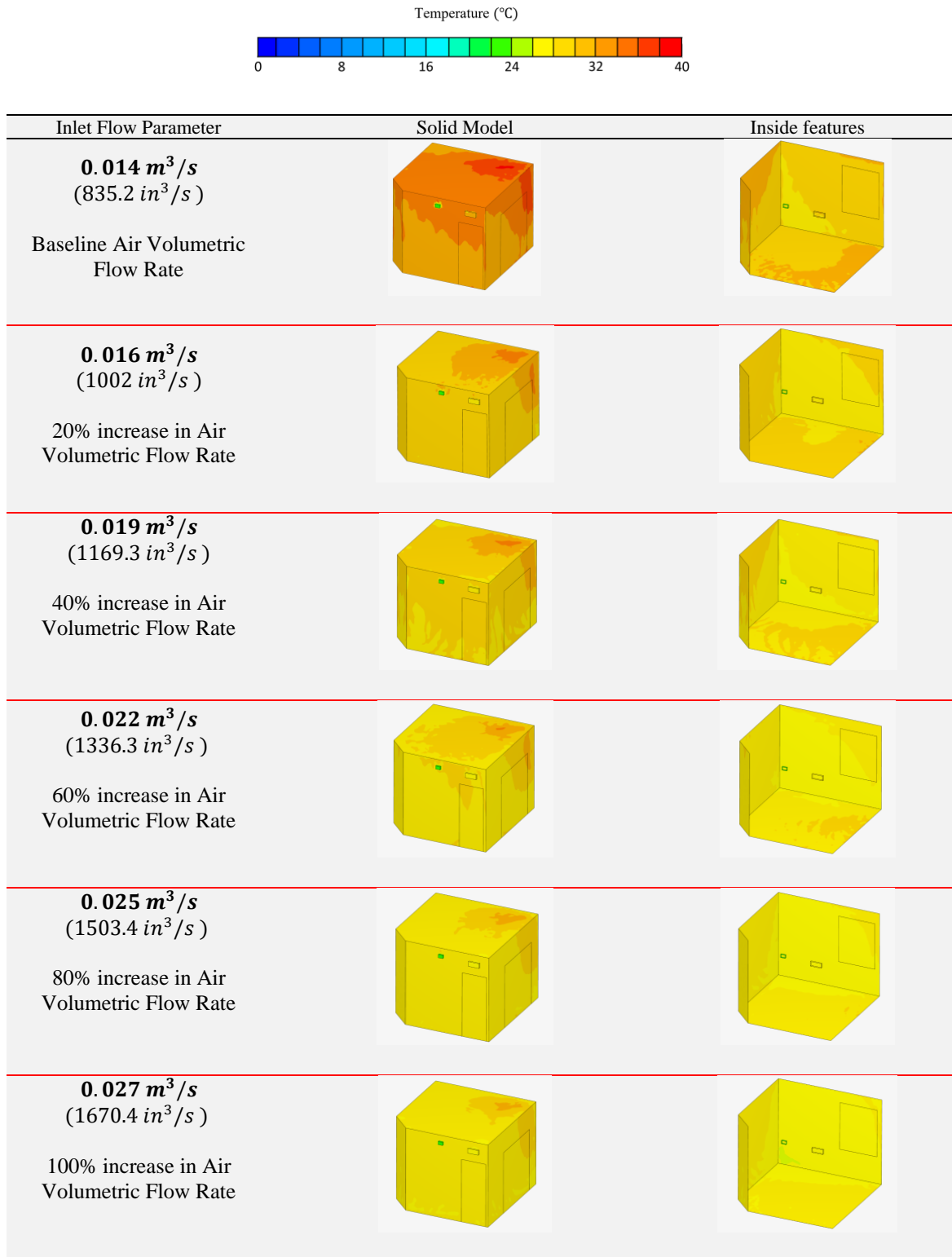


Figure 4.4 Baseline Model Reduced Flow Rates

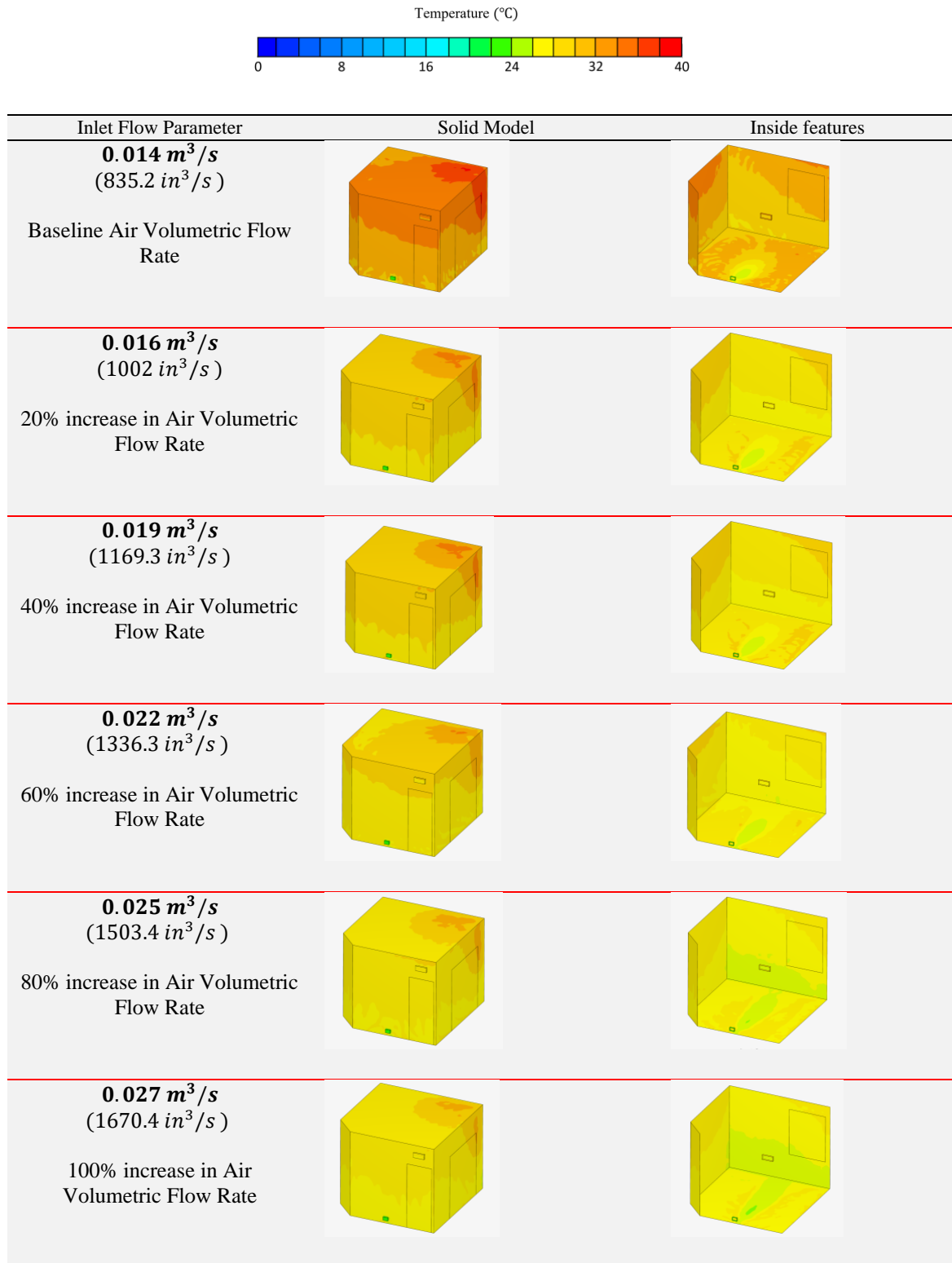


Figure 4.5 Model 1 Reduced Flow Rates

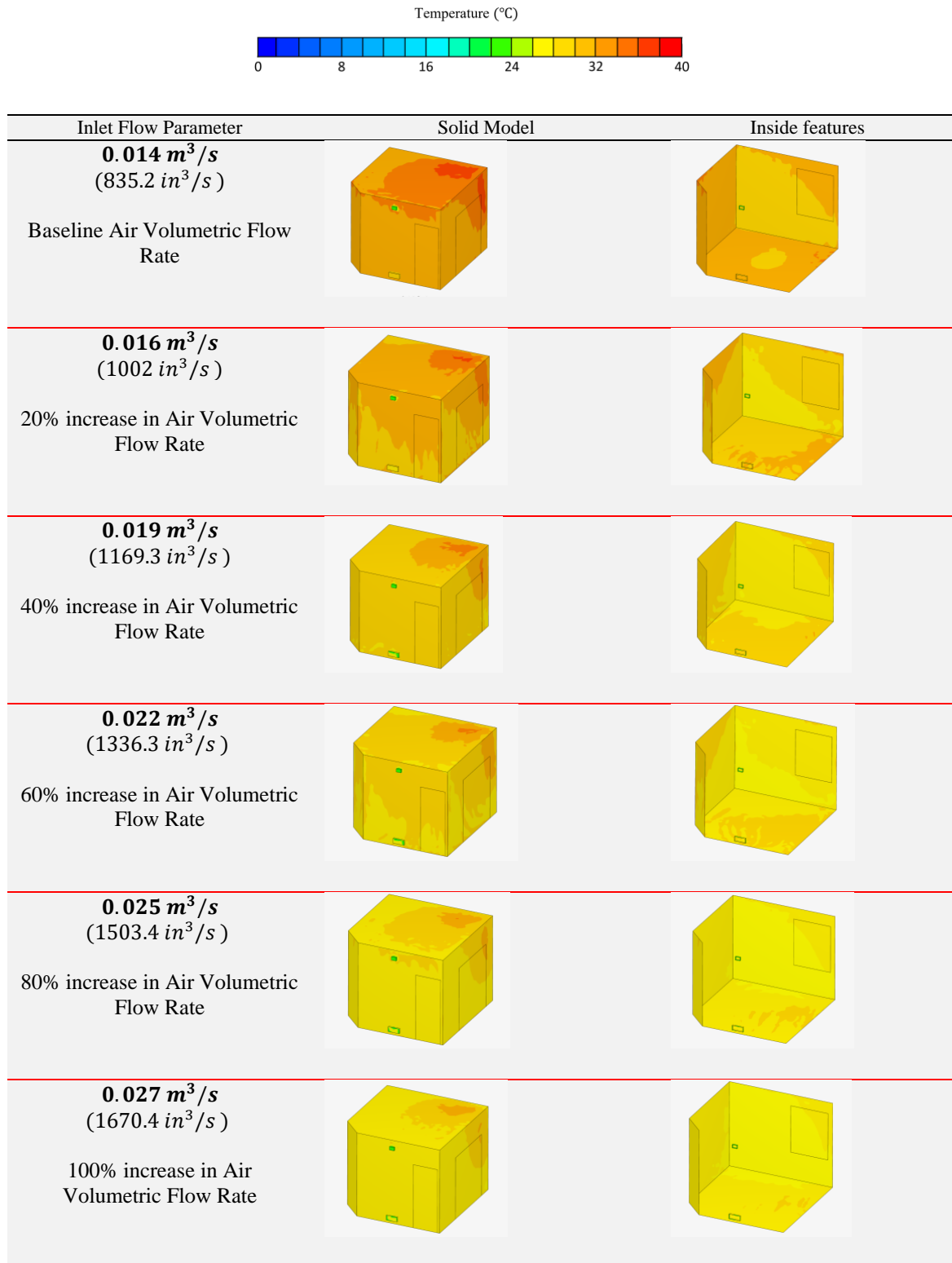


Figure 4.6 Model 2 Reduced Flow Rates

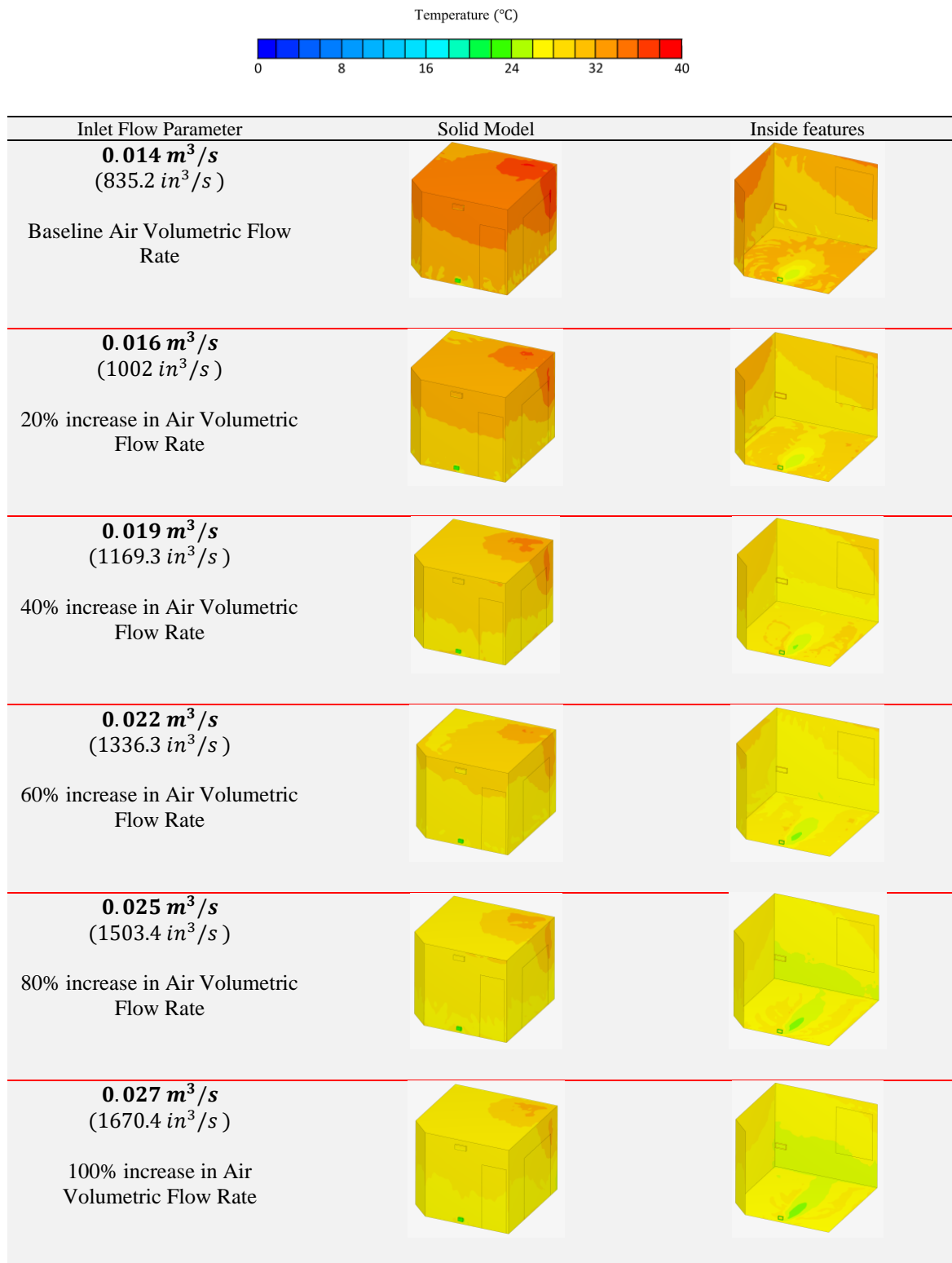


Figure 4.7 Model 3 Reduced Flow Rates



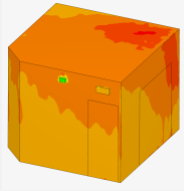
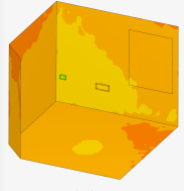
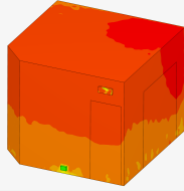
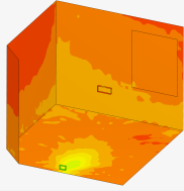
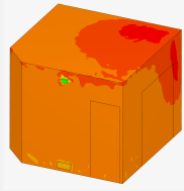
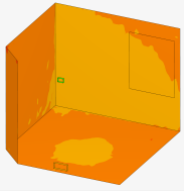
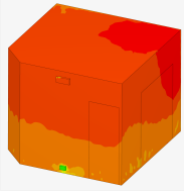
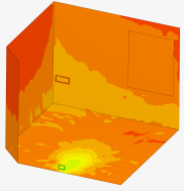
Inlet Flow Parameter	Solid Model	Inside features
Baseline Model		
Model 1		
Model 2		
Model 3		

Figure 4.8 20% decrease in Air Volumetric Flow Rate **0.012  $m^3/s$**  (668.2  $in^3/s$ )

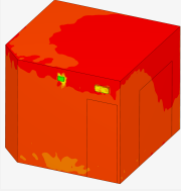
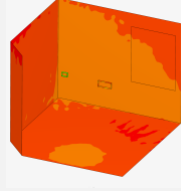
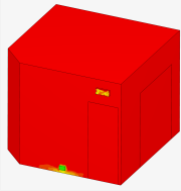
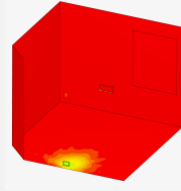
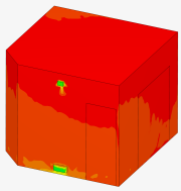
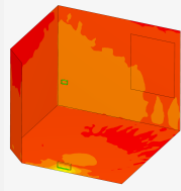
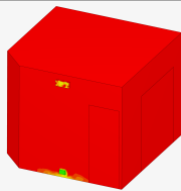
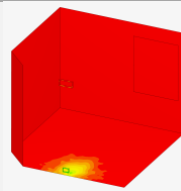
Inlet Flow Parameter	Solid Model	Inside features
Baseline Model		
Model 1		
Model 2		
Model 3		

Figure 4.9 50% decrease in Air Volumetric Flow Rate  $0.0068m^3/s$  ( $417.2\text{ in}^3/s$ )

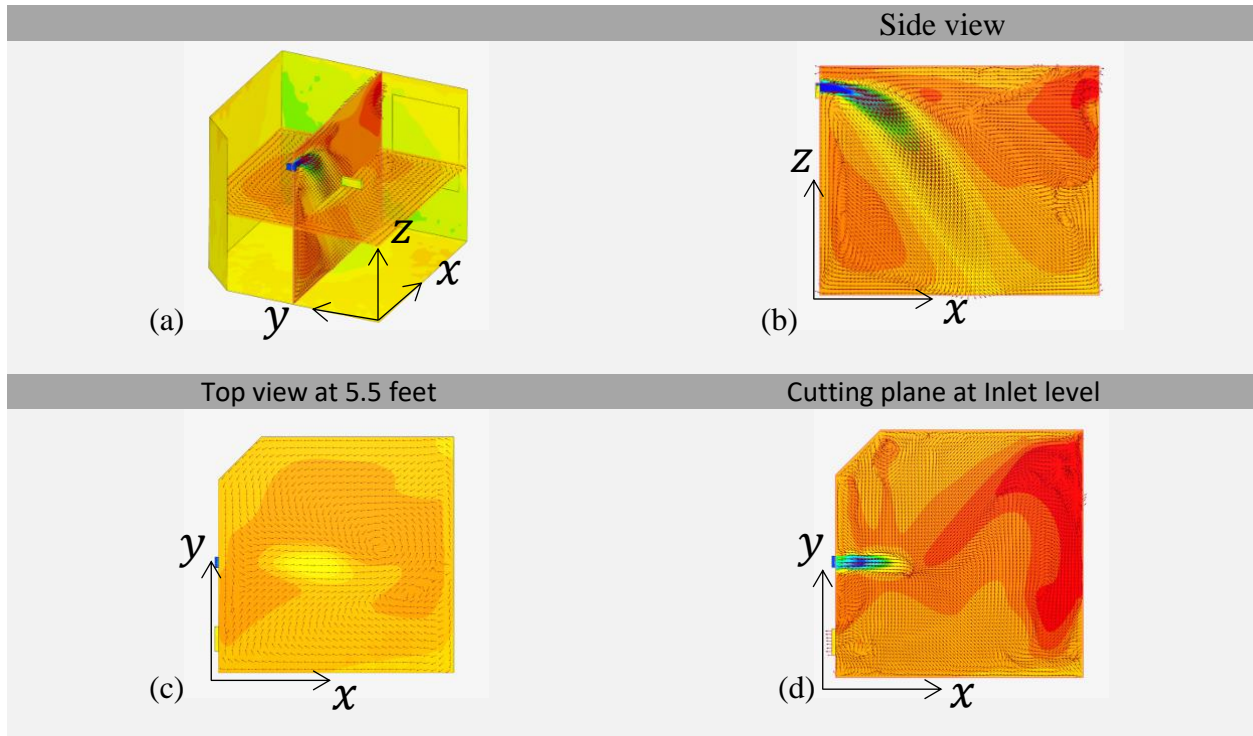


Figure 4.10 Passive Scalar Plot of air conditions (Baseline Model)

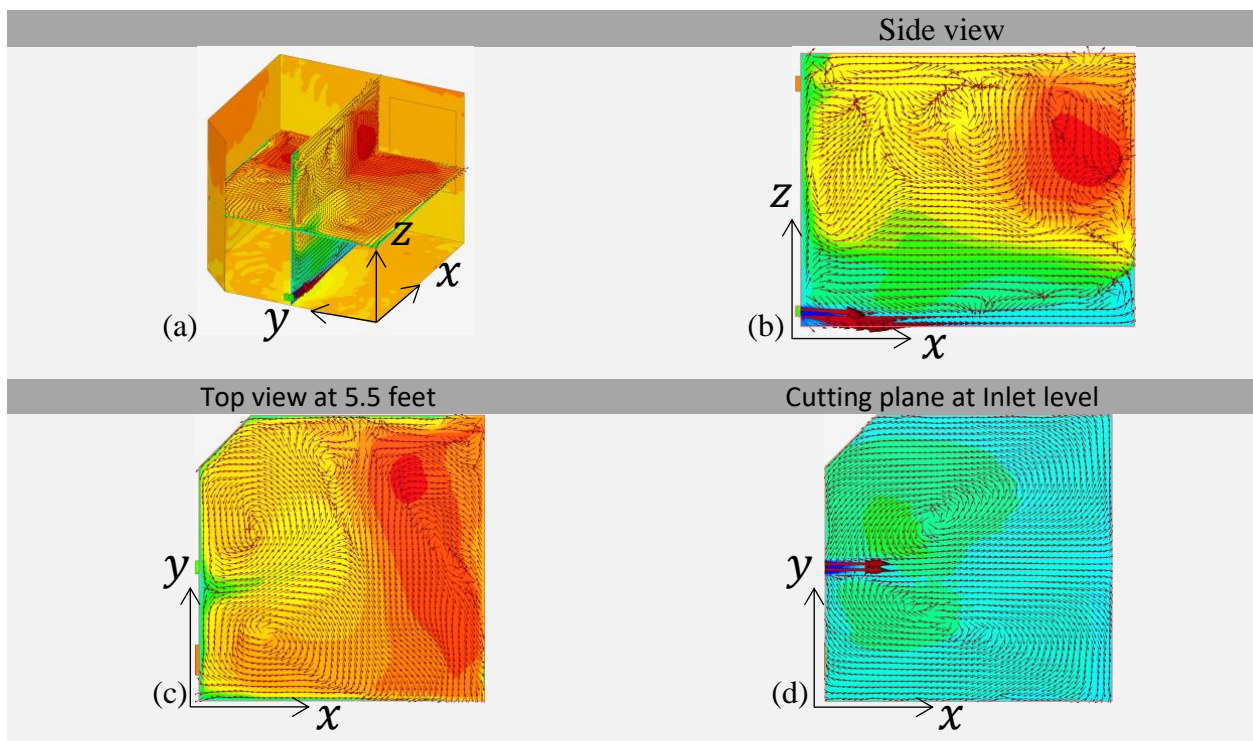


Figure 4.11 Passive Scalar Plot of air conditions (Model 1)

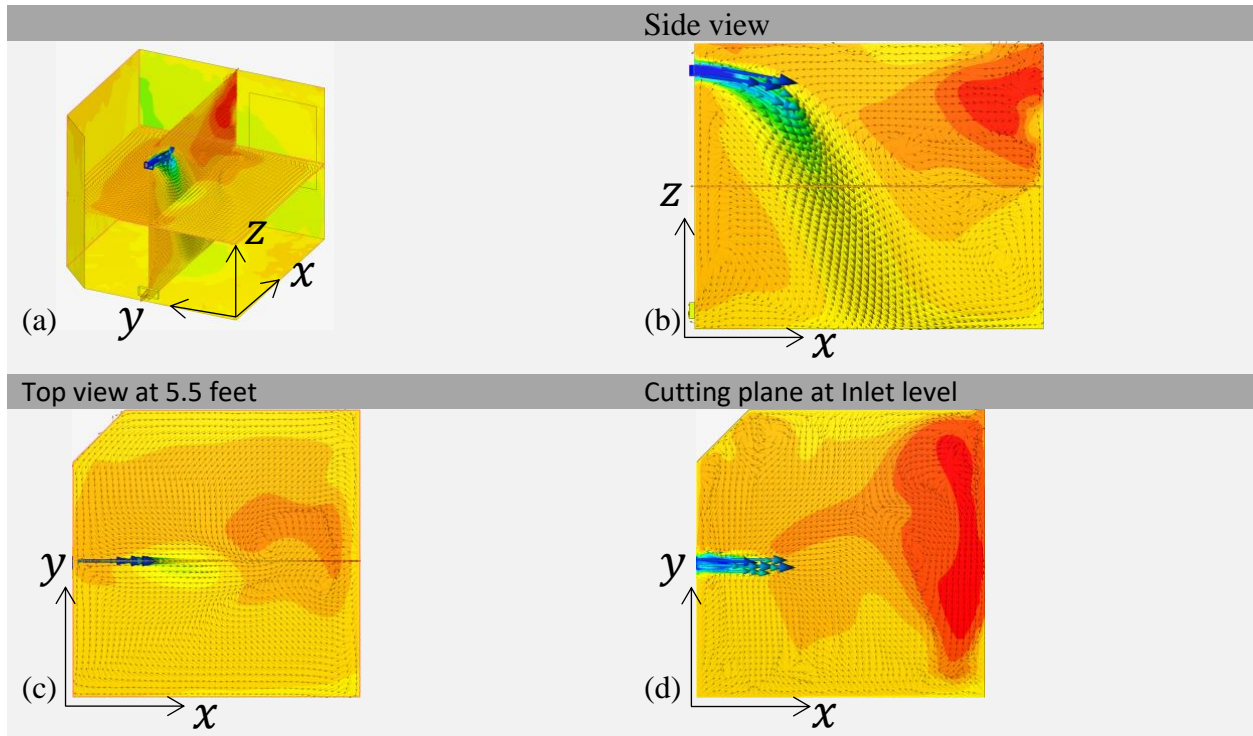


Figure 4.12 Passive Scalar Plot of air conditions (Model 2)

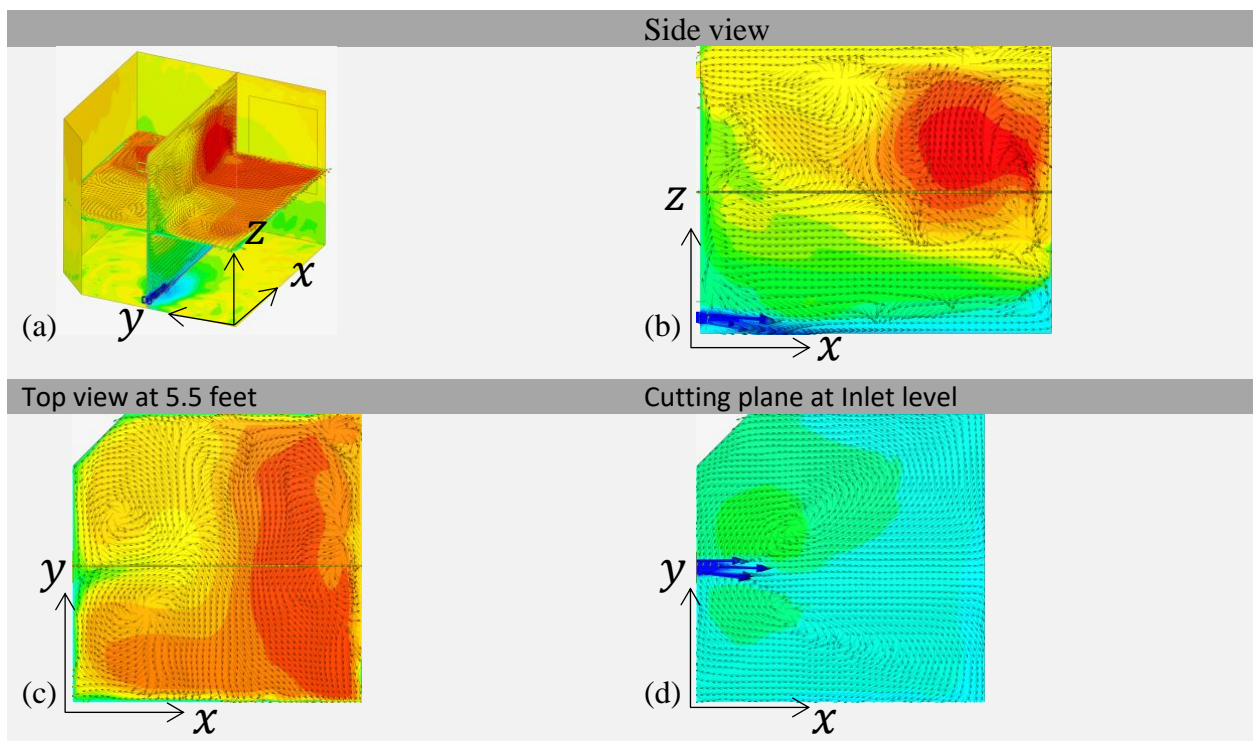


Figure 4.13 Passive Scalar Plot of air conditions (Model 3)

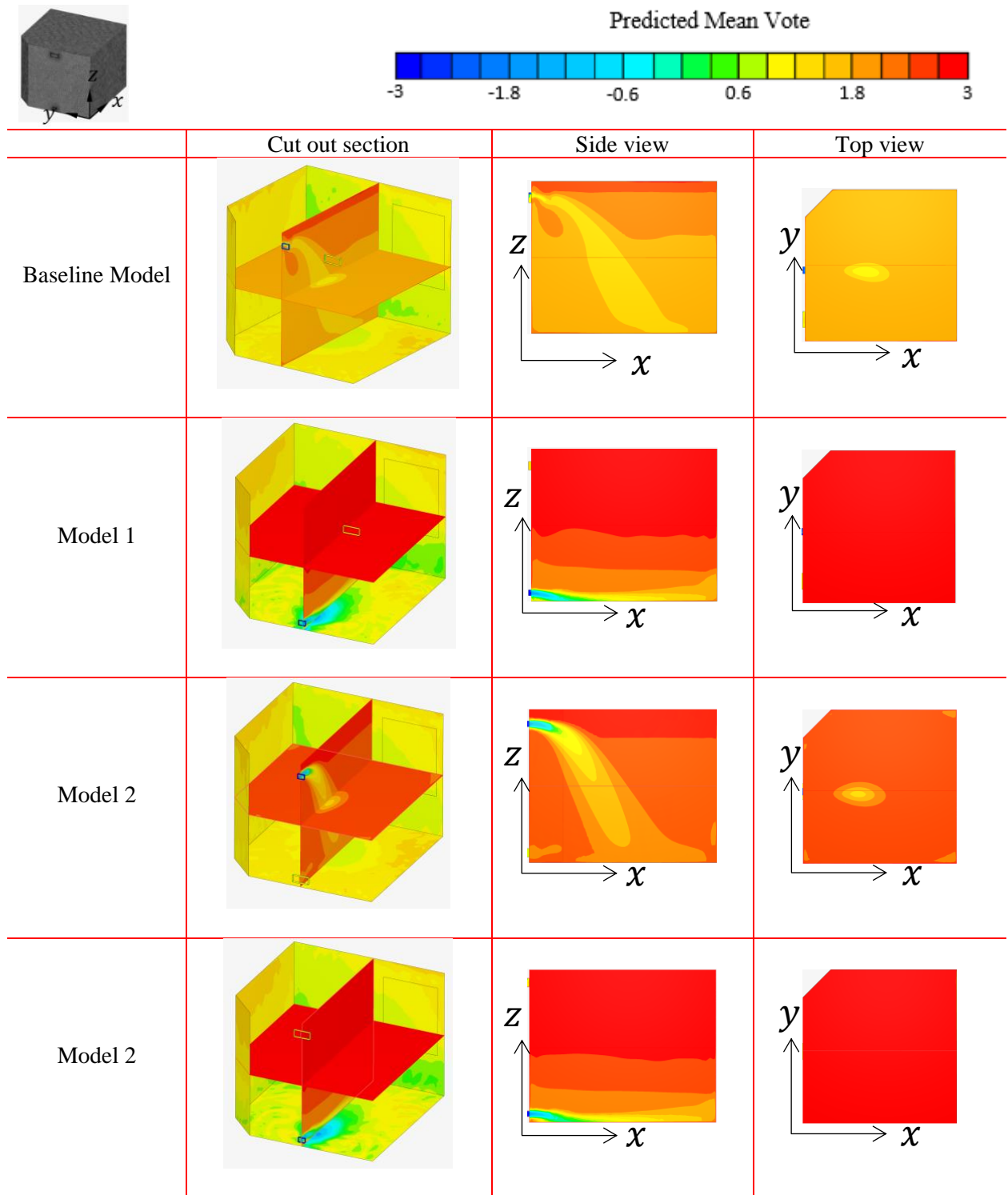


Figure 4.14 Predicted Mean Vote for the Models

#### 4.4 The Local Mean Age of Air

Figures 4.10, 4.11, 4.12 and 4.13 show the passive scalar plots of the baseline model, model 1, model 2 and model 3 respectively. In figure 4.10(a), from Simscale's local mean age of air scale, blue represents fresh air and red represents recirculated air. Green represents an ideal mixture. The side profile for the baseline model figure 4.10(b) shows a section of over circulated air forming at the top right corner of the room. This section extends to the opposite wall, but it expectedly mixes out lightly because its proximity to the inlet vent jet. There is a difference in the passive scalar distribution between the top view profiles at 5.5 feet above the floor (figure 4.10(c)) and at the inlet level (figure 4.10(d)) because the stream of air coming in through the inlet has been designed to not cross the 2 feet occupancy line and therefore, the air "pours" downward into the room. An over circulated section of air can also be seen in model 2 (which is like the baseline model), the recirculated air is less severe in this case and is not as spread out (evident by the small dark red patch in figure 4.12(c)) as in the baseline model. In models 1 and 3, there is an excess amount of fresh air close to the floor of the room. Both sections of fresh air extend for up to 5 feet from the floor. There is also a region of recirculated air noticeable in the top right corner of the side views (figure 4.11(b), figure 4.13(b)). The cutting plane at the inlets of both models (figure 4.11(c), figure 4.13(c)) reveals a smooth blend of fresh and ideal mix of air.

#### 4.5 Thermal Comfort Performance

Figure 4.14 shows the Thermal Comfort Assessment which is based on the Predicted Mean Vote (PMV). The Baseline Model is within the accepted limits of the PMV values in table 3.3. with a max value of approximately +2.5 in the top film section of air. Model 2 also has a section of air which just falls within the bounds of thermal comfort with values of +2 - +3. The top layer,

however, has values above the maximum value of +3. Models 1 and 3 have values beyond the max value. There are, however, comfortable regions below the 5 feet line.

Comparing the passive scalar in results in figures 4.10, 4.11, 4.12 and 4.13 with the PMV plots in figure 4.14 shows that, expectedly, the freshness of air noticed at the lower levels of models 1 and 3 show favorable PMV values of between 0 and +2. The air section above the 5 feet also expectedly, has PMV value above +3. The flow at the low inlet in these models creates turbulence especially at the higher air sections which in turn affects the PMV. The baseline model has PMV values within the ASHRAE accepted range, however, only some sections of model 2 fall within the acceptable range.

#### 4.6 **Conclusions**

The location of air vents was critical to the retention of heat and the buildup of air sections as well as the mixing of air. Air mixing which is an important part of forced air circulation systems contributes to the retention of heat and conservation of energy. When the vents are located at a higher register, the buildup is relatively more homogenous and hence less turbulent. However, this is only guaranteed if the higher register is combined with the “right” flow rate. The flow rate which was used as the baseline ensured a “pouring” effect which contributed to the success of the baseline design. If the flow rate is not at an effective value, the upsides of the high register which include heat retention, slow mixing and less turbulence are no longer ensured. Lower registers heated up the space faster but were more turbulent and less homogenous in distribution. They also help up more fresh air in the control space.

In a real-world system like a house heating system with a thermostat and circulation fans, the lower register provides quicker heating opportunities. Circulation fans could also improve the

mixing and homogeneity of the air sections. In a house system which depends on pressure difference for removal of used up air, the higher register system will work more efficiently.

#### **4.7 Future Work**

The performances of the lower register inlet vents show optimization opportunities. The room is heated up faster than higher register inlet vents. If thermal comfort challenges associated with the lower register inlets can be addressed, then a case can be made for exploring the possibility of an optimized heating system.



## References

1. U.S. Energy Information Administration (2014). *Annual Energy Review 2014*. Washington, DC: U.S. Department of Energy, 2014. Available at: <http://www.eia.gov/forecasts/archive/aeo14/>
2. U.S. Energy Information Administration (2021). *Monthly Energy Review February 2021*. Washington, DC: U.S. Department of Energy. Available at: <https://www.eia.gov/totalenergy/data/monthly/archive/00352102.pdf>
3. Levine, M., D. Ürge-Vorsatz, K. Blok, L. Geng, D. Harvey, S. Lang, G. Levermore, A. Mongameli Mehlwana, S. Mirasgedis, A. Novikova, J. Rilling, H. Yoshino, (2007): *Residential and commercial buildings*. In Climate Change 2007: Mitigation. Contribution of Working Group III to the Fourth Assessment Report of the Intergovernmental Panel on Climate Change [B. Metz, O.R. Davidson, P.R. Bosch, R. Dave, L.A. Meyer (eds)], Cambridge University Press, Cambridge, United Kingdom and New York, NY, USA
4. Stoward P.J. (1962) *Thermodynamics of biological growth*. Nature; 194(4832):977e8. <https://doi.org/10.1038/194977a0>. <https://www.nature.com/articles/194977a0>.
5. Zotin A.Z. (1967). *Thermodynamic aspects of developmental biology*. J Theor Biol; 17(1):57e75. [https://doi.org/10.1016/0022-5193\(67\)90020-3](https://doi.org/10.1016/0022-5193(67)90020-3).
6. Chen, M. (1985). *The tissue energy balance equation*. In : Shitzer, A., Eberhart, R.C.(Eds.), Heat Transfer in Medicine and Biology. Plenum Press, New York, pp.156–157.
7. Psikuta, A., (2009). *Development of an ‘artificial human’ for clothing research*, (PhD thesis). De Montfort University, UK.

8. International Code Council. (2009). *2009 International Energy Conservation Code: Softcover Version (International Code Council Series)* (1st ed.). International Code Council.
9. Division of Building Safety. (2020). *Idaho Statutes and Administrative Rules: Building Statutes Rules Revised*. Retrieved from <https://dbs.idaho.gov/wp-content/uploads/sites/105/2020/12/Building-Statutes-Rules-REVISED.pdf> on 6 March 2021.
10. Idaho Residential Code. (2020). Residential Code for One- and Two-family Dwellings of Idaho. Retrieved from <https://up.codes/viewer/idaho/irc-2018/chapter/1/scope-and-administration#1> on 26 February 2021.
11. International Code Council. (2011). *International Energy Conservation Code 2009*.
12. Burdick A. (2011). Advanced Strategy Guideline: Air Distribution Basics and Duct Design. Report for U.S. Department of Energy; Energy Efficiency & Renewable Energy.
13. American Council for an Energy Efficient Economy. (2021). Types of Heating Systems. Available online: <https://smarterhouse.org/heating-systems/types-heating-systems> accessed on 13 October 2021.
14. Çengel Yunus A., & Ghajar, A. J. (2020). *Heat and mass transfer: Fundamentals & applications*. McGraw-Hill Education.
15. Simscale. (2021a). *Simscale features and benefits*. Available online at <https://www.simscale.com/product/simulation-features/> accessed on 17 October 2021.
16. Simscale. (2021b). *K-Omega and K-Omega SST*. Available online at <https://www.simscale.com/docs/simulation-setup/global-settings/k-omega-sst/> accessed on 17 October 2021.

17. Simscales. (2021c). *Compressible Fluid Flow Analysis*. Available online at <https://www.simscales.com/docs/analysis-types/compressible-fluid-flow-analysis/> accessed on 17 October 2021.
18. Simscales. (2021d). *Incompressible Fluid Flow Analysis*. Available online at <https://www.simscales.com/docs/analysis-types/incompressible-fluid-flow-analysis/> accessed on 17 October 2021.
19. Simscales. (2021e). *Passive Scalar Sources*. Available online at <https://www.simscales.com/docs/simulation-setup/advanced-concepts/passive-scalar-sources/> accessed on 17 October 2021.
20. Simscales. (2021f). *Model Documentation*. Available online at <https://www.simscales.com/docs/simulation-setup/model/> accessed on 17 October 2021.
21. Simscales. (2021g). *Thermal Comfort Parameters*. Available online at <https://simscales.staging.wpengine.com/docs/simulation-setup/result-control/thermal-comfort-parameters/> accessed on 21 October 2021
22. Jenkins M. (2020). *What is ASHRAE 55? Basics of Thermal Comfort*. Available online at <https://www.simscales.com/blog/2019/08/what-is-ashrae-55-thermal-comfort/> accessed on 17 October 2021. Report for Simscales.
23. ASHRAE (2020). *Standard 55 – Thermal Environmental Conditions for Human Occupancy*. Available online at <https://www.ashrae.org/technical-resources/bookstore/standard-55-thermal-environmental-conditions-for-human-occupancy> accessed on 21 October 2021.

24. Simscale. (2021h). *What is a Mesh?*. Available online at <https://www.simscale.com/docs/simwiki/preprocessing/what-is-a-mesh/> accessed on 21 October 2021
25. Simscale. (2021i). *Standard Mesher*. Available online at <https://www.simscale.com/docs/simulation-setup/meshing/standard/> accessed on 21 October 2021
26. Simscale. (2021j). *Why OpenFOAM Users Should Try Simscale*. Available online at <https://www.simscale.com/blog/2016/10/openfoam-users-should-try-simscale/> accessed on 21 October 2021
27. OpenCFD. (2021). *About ESI-CFD*. Available online at <https://www.openfoam.com/about-esi-opencfd> accessed on 21 October 2021
28. Buratti, C. & Vergoni, M. & Palladino, Domenico. (2015). *Thermal Comfort Evaluation Within Non-residential Environments: Development of Artificial Neural Network by Using the Adaptive Approach Data*. *Energy Procedia*. 78. 2875-2880. 10.1016/j.egypro.2015.11.656.
29. Oezcan M. (2020). *How to Assign Wall and Window Settings for Thermal Comfort Simulations*. Available online at <https://www.simscale.com/knowledge-base/how-to-assign-wall-and-window-settings-for-thermal-comfort-simulations/> accessed on 17 October 2021. Report for Simscale.
30. Engineering ToolBox, (2003). *Thermal Conductivity Coefficients for common Solids, Liquids and Gases*. [online] Available at: [https://www.engineeringtoolbox.com/thermal-conductivity-d\\_429.html](https://www.engineeringtoolbox.com/thermal-conductivity-d_429.html) accessed 23 July 2021

31. TenWolde A., McNatt J. D., Krahm L. (1988). *Thermal Properties of Wood and Wood Panel Products for use in Buildings*. Part of The National Program for Building Thermal Envelope Systems and Materials. Prepared for the U.S. Department of Energy Conservation and Renewable Energy Office of Buildings and Community Systems Building Systems Division.
32. Igaz R., Krišáka L., Ružiak I., Gajtanska M., and Kučerka M. (2017). *Thermophysical Properties of OSB Boards versus Equilibrium Moisture Content*. BioResources 12(4), 8106-8118
33. ASHRAE (2017). *ANSI/ASHRAE Standard 55: Thermal Environmental Conditions for Human Occupancy*. Atlanta: American Society of Heating, Refrigerating and Air Conditioning Engineers.

## Appendix A: Standard Window Dimensions

### 100 SERIES GLIDING WINDOWS

Andersen®

**Table of Gliding Window Sizes – Active-Stationary or Stationary-Active (X0/OX)**

Scale 1/8" (3) = 1'-0" (305) – 1:96

Window Dimension	1'-11 1/2"	2'-5 1/2"	2'-11 1/2"	3'-5 1/2"	3'-11 1/2"	4'-5 1/2"	4'-11 1/2"	5'-5 1/2"	5'-11 1/2"
	(597)	(749)	(902)	(1054)	(1207)	(1359)	(1511)	(1664)	(1816)
<b>Minimum Rough Opening</b>	2'-0"	2'-6"	3'-0"	3'-6"	4'-0"	4'-6"	5'-0"	5'-6"	6'-0"
	(610)	(762)	(914)	(1067)	(1219)	(1372)	(1524)	(1676)	(1829)
Unobstructed Glass (width of single sash)	7 9/16"	10 9/16"	13 9/16"	16 9/16"	19 9/16"	22 9/16"	25 9/16"	28 9/16"	31 9/16"
	(192)	(268)	(344)	(420)	(496)	(573)	(649)	(725)	(801)

CUSTOM WIDTHS – 23 1/2" to 71 1/2"									
11 1/2"	2010	2610	3010	3610	4010	4610	5010	5610	6010
1'-5 1/2"	2016	2616	3016	3616	4016	4616	5016	5616	6016
1'-11 1/2"	2020	2620	3020	3620	4020	4620	5020	5620	6020
2'-5 1/2"	2026	2626	3026	3626	4026	4626	5026	5626	6026 <sup>9</sup>
2'-11 1/2"	2030	2630	3030	3630	4030	4630	5030 <sup>9</sup>	5630 <sup>9</sup>	6030 <sup>9</sup>
3'-5 1/2"	2036	2636	3036	3636	4036	4636 <sup>9</sup>	5036 <sup>9</sup>	5636 <sup>9</sup>	6036 <sup>9</sup>
3'-11 1/2"	2040	2640	3040	3640	4040 <sup>9</sup>	4640 <sup>9</sup>	5040 <sup>9</sup>	5640 <sup>9</sup>	6040 <sup>9</sup>
4'-5 1/2"	2046	2646	3046	3646	4046 <sup>9</sup>	4646 <sup>9</sup>	5046 <sup>9</sup>	5646 <sup>9</sup>	6046 <sup>9</sup>
4'-11 1/2"	2050	2650	3050	3650	4050 <sup>9</sup>	4650 <sup>9</sup>	5050 <sup>9</sup>	5650 <sup>9</sup>	6050 <sup>9</sup>
5'-5 1/2"	2056	2656	3056	3656	4056 <sup>9</sup>	4656 <sup>9</sup>	5056 <sup>9</sup>	5656 <sup>9</sup>	6056 <sup>9</sup>
5'-11 1/2"	2060	2660	3060	3660	4060 <sup>9</sup>	4660 <sup>9</sup>	5060 <sup>9</sup>	5660 <sup>9</sup>	6060 <sup>9</sup>



Custom-size windows are available  
in 1/8" (3) increments.



Active-Stationary



Stationary-Active

Choose active-stationary (X0) or stationary-active (OX)  
as viewed from the exterior. Two locks are standard on all  
heights greater than 4'-2" (1270).

\* "Window Dimension" always refers to outside frame to frame dimension.  
\*\* "Minimum Rough Opening" dimensions may need to be increased to allow for use of building wraps, flashing, sill panning, brackets, fasteners or other items.  
† Dimensions in parentheses are in millimeters.  
‡ Meet or exceed clear opening area of 5.7 sq.ft. or 0.53 m<sup>2</sup>, clear opening width of 20" (508) and clear opening height of 24" (610).

100 SERIES GLIDING WINDOWS

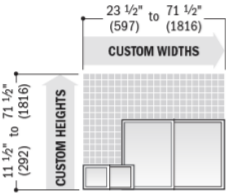


Custom Sizes & Specifications

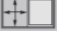

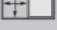



100 Series custom-size windows are available in 1/8" (3) increments between minimum and maximum widths and heights shown. Some restrictions apply.

Gliding Windows



Active-Stationary or Stationary-Active (X0/OX)

<b>Clear Opening</b>  Width = (window width + 2) - 3.711" (94) Height = window height - 3.500" (89)	<b>Minimum R.O.</b>  Width = window width + 1/2" (13) Height = window height + 1/2" (13)
<b>Vent Opening</b>  Width = (window width + 2) - 3.711" (94) Height = window height - 3.500" (89)	<b>Unobstr. Glass</b>  Fixed Sash Width = (window width + 2) - 4.184" (106) Venting Sash Width = (window width + 2) - 4.226" (107) Total Sash Width = window width - 8.410" (214) Height = window height - 6.250" (159)

## Appendix B: Standard Patio Door Dimensions

### 400 SERIES FRENCHWOOD® HINGED INSWING PATIO DOORS



**Table of Frenchwood® Hinged Inswing Patio Door Sizes**

Scale 1/8" (3) = 1'-0" (305) – 1:96

Door Dimension	2'-0 1/2"			4'-0"	4'-0"			
	(620)			(1219)	(1219)			
Minimum Rough Opening	2'-1"			4'-1"	4'-1"			(patio door heights on the next page)
	(634)			(1242)	(1242)			
Unobstructed Glass (single panel only)	13 1/4"			13 1/4"	13 1/4"			
	(336)			(336)	(336)			
3 heights								
	<b>1</b> FWH2168S <b>2</b> FWH21611S <b>3</b> FWH2180S			FWH4168APLR FWH41611APLR FWH4180APLR	FWH4168PALR FWH41611PALR FWH4180PALR			
Door Dimension	2'-6 1/8"	2'-6 1/8"	2'-6 1/8"	4'-11 1/4"	4'-11 1/4"	4'-11 1/4"	4'-11 1/4"	4'-11 1/4"
	(765)	(765)	(765)	(1504)	(1504)	(1504)	(1504)	(1504)
Minimum Rough Opening	2'-7"	2'-7"	2'-7"	5'-0"	5'-0"	5'-0"	5'-0"	5'-0"
	(787)	(787)	(787)	(1524)	(1524)	(1524)	(1524)	(1524)
Unobstructed Glass (single panel only)	18 7/8"	18 7/8"	18 7/8"	18 7/8"	18 7/8"	18 7/8"	18 7/8"	18 7/8"
	(479)	(479)	(479)	(479)	(479)	(479)	(479)	(479)
3 heights								
	<b>1</b> FWH2768S <b>2</b> FWH27611S <b>3</b> FWH2780S	FWH2768AR FWH27611AR FWH2780AR	FWH2768AL FWH27611AL FWH2780AL	FWH5068SS FWH50611SS FWH5080SS	FWH5068ASR FWH50611ASR FWH5080ASR	FWH5068SAL FWH50611SAL FWH5080SAL	FWH5068APLR FWH50611APLR FWH5080APLR	FWH5068PALR FWH50611PALR FWH5080PALR
Door Dimension	2'-8 1/8"	2'-8 1/8"	2'-8 1/8"	5'-3 1/4"	5'-3 1/4"	5'-3 1/4"	5'-3 1/4"	5'-3 1/4"
	(816)	(816)	(816)	(1607)	(1607)	(1607)	(1607)	(1607)
Minimum Rough Opening	2'-9"	2'-9"	2'-9"	5'-4"	5'-4"	5'-4"	5'-4"	5'-4"
	(838)	(838)	(838)	(1626)	(1626)	(1626)	(1626)	(1626)
Unobstructed Glass (single panel only)	20 7/8"	20 7/8"	20 7/8"	20 7/8"	20 7/8"	20 7/8"	20 7/8"	20 7/8"
	(530)	(530)	(530)	(530)	(530)	(530)	(530)	(530)
3 heights								
	<b>1</b> FWH2968S <b>2</b> FWH29611S <b>3</b> FWH2980S	FWH2968AR FWH29611AR FWH2980AR	FWH2968AL FWH29611AL FWH2980AL	FWH5468SS FWH54611SS FWH5480SS	FWH5468ASR FWH54611ASR FWH5480ASR	FWH5468SAL FWH54611SAL FWH5480SAL	FWH5468APLR FWH54611APLR FWH5480APLR	FWH5468PALR FWH54611PALR FWH5480PALR
Door Dimension	3'-0 1/8"	3'-0 1/8"	3'-0 1/8"	5'-11 1/4"	5'-11 1/4"	5'-11 1/4"	5'-11 1/4"	5'-11 1/4"
	(918)	(918)	(918)	(1810)	(1810)	(1810)	(1810)	(1810)
Minimum Rough Opening	3'-1"	3'-1"	3'-1"	6'-0"	6'-0"	6'-0"	6'-0"	6'-0"
	(940)	(940)	(940)	(1829)	(1829)	(1829)	(1829)	(1829)
Unobstructed Glass (single panel only)	24 7/8"	24 7/8"	24 7/8"	24 7/8"	24 7/8"	24 7/8"	24 7/8"	24 7/8"
	(632)	(632)	(632)	(632)	(632)	(632)	(632)	(632)
3 heights								
	<b>1</b> FWH3168S <b>2</b> FWH31611S <b>3</b> FWH3180S	FWH3168AR FWH31611AR FWH3180AR	FWH3168AL FWH31611AL FWH3180AL	FWH6068SS FWH60611SS FWH6080SS	FWH6068ASR FWH60611ASR FWH6080ASR	FWH6068SAL FWH60611SAL FWH6080SAL	FWH6068APLR FWH60611APLR FWH6080APLR	FWH6068PALR FWH60611PALR FWH6080PALR

\* "Door Dimension" always refers to outside frame-to-frame dimension.

\*\* "Minimum Rough Opening" dimensions may need to be increased to allow for use of building wraps, flashing, sill panning, brackets, fasteners or other items.

\* Dimensions in parentheses are in millimeters.

2021-22 400 Series Product Guide



Custom-size doors are available in 1/8" (3) increments.

Stationary (S) doors can be used as an individual unit or as a sidelight. In addition to venting door panels shown in table, other standard configurations are available for two- and three-panel doors.

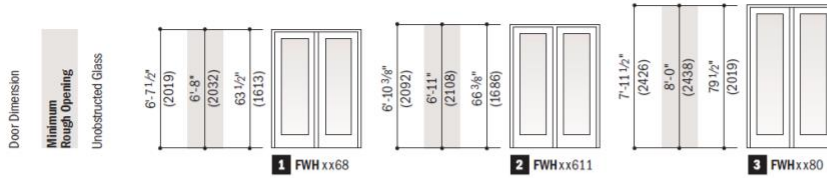
(continued)



## 400 SERIES FRENCHWOOD® HINGED INSWING PATIO DOORS

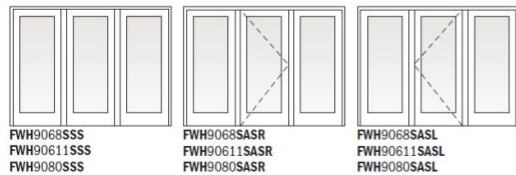
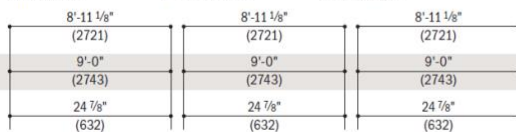
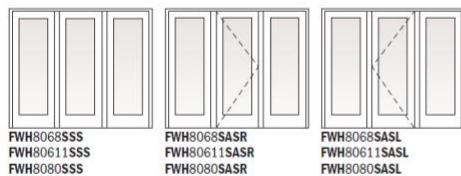
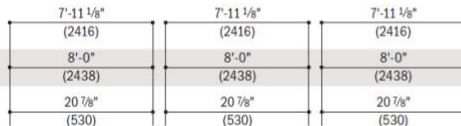
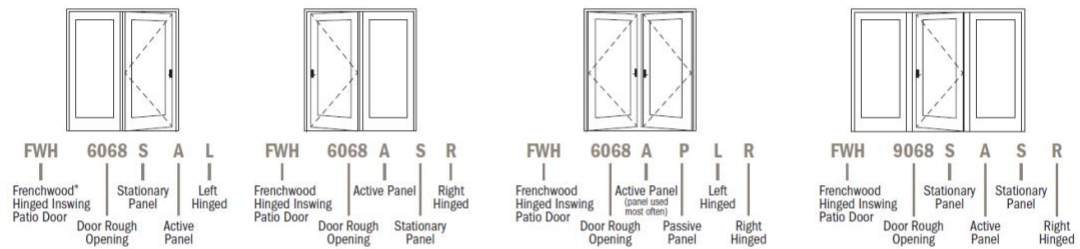


### Three Patio Door Heights



### Order Designation Description

Viewed from the exterior.

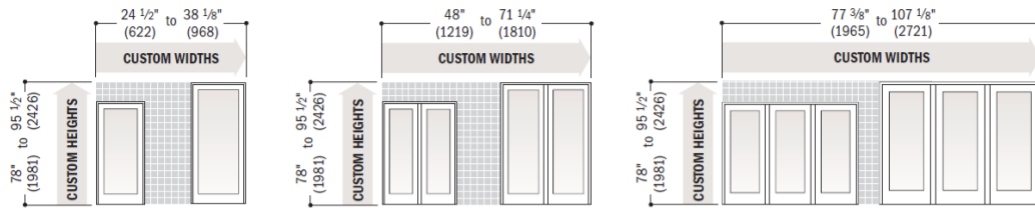


\* "Door Dimension" always refers to outside frame-to-frame dimension.  
 \* "Minimum Rough Opening" dimensions may need to be increased to allow for use of building wraps, flashing, sill panning, brackets, fasteners or other items.  
 \* Dimensions in parentheses are in millimeters.

## 400 SERIES FRENCHWOOD® HINGED INSWING PATIO DOORS



### Custom Sizes and Specification Formulas



Clear Opening	Height = height - 4.22" (107)	Minimum R.O.	Width = width + 3/4" (19) Height = height + 1/2" (13)	Unobst. Glass	Single-Panel Width = width - 11.22" (285) Height = height - 16.05" (408) Two-Panel Width = width - 21.5" (546) Height = height - 16.05" (408) Three-Panel Width = width - 32.55" (827) Height = height - 16.05" (408)
 	<b>Single-Panel</b> Width = width - 5.744" (145)  <b>Two-Panel, two panels open</b> Width = width - 7.394" (187)  <b>Two-Panel, one panel open</b> Width = (width - 10.550" (267)) + 2  <b>Three-Panel</b> Width = (width - 16.106" (409)) + 3				

\* Clear opening width formulas are based on panel(s) in a 90° open position.

\* Dimensions in parentheses are in millimeters.

\* **Clear Opening** formulas provide dimensions for determining area available for egress. Vent opening, or area available for passage of air, is equal to clear opening. **Minimum R.O.** (minimum rough opening) formulas provide minimum rough opening width and height dimensions. **Unobst. Glass** (unobstructed glass) formulas provide dimensions for determining area available for passage of light.



Available in 1/8" (3) increments between minimum and maximum widths and heights. Some restrictions apply. Measurement guide can be found at [andersenwindows.com/measure](http://andersenwindows.com/measure).

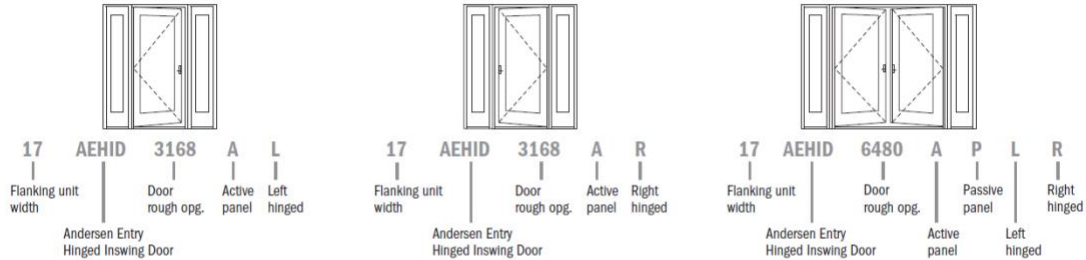
## Appendix C: Standard Entry Door Dimensions

### ENTRY DOORS



#### Order Designation Description

Viewed from the exterior.



Inswing entry doors (AEHID) shown above, for outswing entry doors use AEOD. Outswing entry doors open outward to the exterior.



Custom-size doors are available in 1/8" (3) increments.

Available in custom designed panels. Stationary doors are also available (i.e. AEHID2068S or AEHID4068SS).

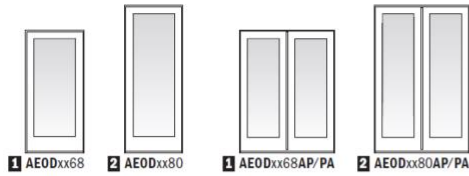
#### Rectangular Inswing Entry Door Dimensions and Specifications

Door Number	Number of Panels Open*	Min. Rough Opening				Clear Opening Maximums						Overall Door Area Sq. Ft./ (m <sup>2</sup> )
		Width Inches/(mm)	Height Inches/(mm)	Width Inches/(mm)	Height Inches/(mm)	Clear Opening Sq. Ft./ (m <sup>2</sup> )	90° Width Inches/(mm)	Full Width Inches/(mm)	Height Inches/(mm)			
AEHID2068	1	25 1/8" (652)	82" (2083)	26 1/8" (665)	82 1/2" (2096)	12.56 (1.17)	20 1/8" (529)	22 1/8" (581)	79 1/8" (2008)	12.56 (1.17)	14.63 (1.36)	
AEHID2668	1	31 1/8" (805)	82" (2083)	32 1/8" (818)	82 1/2" (2096)	15.85 (1.47)	26 1/8" (681)	28 1/8" (733)	79 1/8" (2008)	15.85 (1.47)	18.04 (1.68)	
AEHID2868	1	33 1/8" (856)	82" (2083)	34 1/8" (868)	82 1/2" (2096)	16.95 (1.57)	28 1/8" (732)	30 1/8" (784)	79 1/8" (2008)	16.95 (1.57)	19.18 (1.78)	
AEHID3068	1	37 1/8" (957)	82" (2083)	38 1/8" (970)	82 1/2" (2096)	19.15 (1.78)	32 1/8" (833)	34 1/8" (886)	79 1/8" (2008)	19.15 (1.78)	21.46 (1.99)	
AEHID3668	1	43 1/8" (1110)	82" (2083)	44 1/8" (1122)	82 1/2" (2096)	22.44 (2.08)	38 1/8" (986)	40 1/8" (1038)	79 1/8" (2008)	22.44 (2.08)	24.88 (2.31)	
AEHID2080	1	25 1/8" (652)	95" (2413)	26 1/8" (665)	95 1/2" (2426)	14.62 (1.36)	20 1/8" (529)	22 1/8" (581)	92 1/8" (2338)	14.62 (1.36)	16.95 (1.57)	
AEHID2680	1	31 1/8" (805)	95" (2413)	32 1/8" (818)	95 1/2" (2426)	18.46 (1.71)	26 1/8" (681)	28 1/8" (733)	92 1/8" (2338)	18.46 (1.71)	20.90 (1.94)	
AEHID2880	1	33 1/8" (856)	95" (2413)	34 1/8" (868)	95 1/2" (2426)	19.74 (1.83)	28 1/8" (732)	30 1/8" (784)	92 1/8" (2338)	19.74 (1.83)	22.22 (2.06)	
AEHID3080	1	37 1/8" (957)	95" (2413)	38 1/8" (970)	95 1/2" (2426)	22.30 (2.07)	32 1/8" (833)	34 1/8" (886)	92 1/8" (2338)	22.30 (2.07)	24.86 (2.31)	
AEHID3680	1	43 1/8" (1110)	95" (2413)	44 1/8" (1122)	95 1/2" (2426)	26.13 (2.43)	38 1/8" (986)	40 1/8" (1038)	92 1/8" (2338)	26.13 (2.43)	28.82 (2.68)	
AEHID4068	2	50 1/8" (1289)	82" (2083)	51 1/8" (1302)	82 1/2" (2096)	26.32 (2.45)	43 1/8" (1113)	47 1/8" (1218)	79 1/8" (2008)	26.32 (2.45)	28.90 (2.68)	
AEHID4068	1	50 3/8" (1289)	82" (2083)	51 1/8" (1302)	82 1/2" (2096)	12.59 (1.17)	20 1/8" (530)	22 1/8" (583)	79 1/8" (2008)	12.59 (1.17)	28.90 (2.68)	
AEHID5068	2	62 1/8" (1594)	82" (2083)	63 1/8" (1607)	82 1/2" (2096)	32.91 (3.06)	55 1/8" (1418)	59 1/8" (1522)	79 1/8" (2008)	32.91 (3.06)	35.73 (3.32)	
AEHID5068	1	62 1/8" (1594)	82" (2083)	63 1/8" (1607)	82 1/2" (2096)	15.89 (1.48)	26 1/8" (683)	28 1/8" (735)	79 1/8" (2008)	15.89 (1.48)	35.73 (3.32)	
AEHID5468	2	66 1/8" (1695)	82" (2083)	67 1/8" (1708)	82 1/2" (2096)	35.10 (3.26)	59 1/8" (1519)	63 1/8" (1624)	79 1/8" (2008)	35.10 (3.26)	38.01 (3.53)	
AEHID5468	1	66 1/8" (1695)	82" (2083)	67 1/8" (1708)	82 1/2" (2096)	16.99 (1.58)	28 1/8" (733)	30 1/8" (786)	79 1/8" (2008)	16.99 (1.58)	38.01 (3.53)	
AEHID6068	2	74 1/8" (1899)	82" (2083)	75 1/8" (1911)	82 1/2" (2096)	39.50 (3.67)	67 1/8" (1722)	71 1/8" (1827)	79 1/8" (2008)	39.50 (3.67)	42.57 (3.95)	
AEHID6068	1	74 1/8" (1899)	82" (2083)	75 1/8" (1911)	82 1/2" (2096)	19.18 (1.78)	32 1/8" (835)	34 1/8" (887)	79 1/8" (2008)	19.18 (1.78)	42.57 (3.95)	
AEHID7068	2	86 1/8" (2203)	82" (2083)	87 1/8" (2216)	82 1/2" (2096)	46.09 (4.28)	79 1/8" (2027)	83 1/8" (2132)	79 1/8" (2008)	46.09 (4.28)	49.40 (4.59)	
AEHID7068	1	86 1/8" (2203)	82" (2083)	87 1/8" (2216)	82 1/2" (2096)	22.48 (2.09)	38 1/8" (987)	40 1/8" (1040)	79 1/8" (2008)	22.48 (2.09)	49.40 (4.59)	
AEHID4080	2	50 1/8" (1289)	95" (2413)	51 1/8" (1302)	95 1/2" (2426)	30.65 (2.85)	43 1/8" (1113)	47 1/8" (1218)	92 1/8" (2338)	30.65 (2.85)	33.48 (3.11)	
AEHID4080	1	50 1/8" (1289)	95" (2413)	51 1/8" (1302)	95 1/2" (2426)	14.66 (1.36)	20 1/8" (530)	22 1/8" (583)	92 1/8" (2338)	14.66 (1.36)	33.48 (3.11)	
AEHID5080	2	62 1/8" (1594)	95" (2413)	63 1/8" (1607)	95 1/2" (2426)	38.32 (3.56)	55 1/8" (1418)	59 1/8" (1522)	92 1/8" (2338)	38.32 (3.56)	41.40 (3.85)	
AEHID5080	1	62 1/8" (1594)	95" (2413)	63 1/8" (1607)	95 1/2" (2426)	18.50 (1.72)	26 1/8" (683)	28 1/8" (735)	92 1/8" (2338)	18.50 (1.72)	41.40 (3.85)	
AEHID5480	2	66 1/8" (1695)	95" (2413)	67 1/8" (1708)	95 1/2" (2426)	40.88 (3.80)	59 1/8" (1519)	63 1/8" (1624)	92 1/8" (2338)	40.88 (3.80)	44.04 (4.09)	
AEHID5480	1	66 1/8" (1695)	95" (2413)	67 1/8" (1708)	95 1/2" (2426)	19.78 (1.84)	28 1/8" (733)	30 1/8" (786)	92 1/8" (2338)	19.78 (1.84)	44.04 (4.09)	
AEHID6080	2	74 1/8" (1899)	95" (2413)	75 1/8" (1911)	95 1/2" (2426)	45.99 (4.27)	67 1/8" (1722)	71 1/8" (1827)	92 1/8" (2338)	45.99 (4.27)	49.31 (4.58)	
AEHID6080	1	74 1/8" (1899)	95" (2413)	75 1/8" (1911)	95 1/2" (2426)	22.34 (2.08)	32 1/8" (835)	34 1/8" (887)	92 1/8" (2338)	22.34 (2.08)	49.31 (4.58)	
AEHID7080	2	86 1/8" (2203)	95" (2413)	87 1/8" (2216)	95 1/2" (2426)	53.66 (4.99)	79 1/8" (2027)	83 1/8" (2132)	92 1/8" (2338)	53.66 (4.99)	57.23 (5.32)	
AEHID7080	1	86 1/8" (2203)	95" (2413)	87 1/8" (2216)	95 1/2" (2426)	26.17 (2.43)	38 1/8" (987)	40 1/8" (1040)	92 1/8" (2338)	26.17 (2.43)	57.23 (5.32)	

- \* "Door Dimension" always refers to outside frame to frame dimension.
- \* "Minimum Rough Opening" dimensions may need to be increased to allow for use of building wraps, flashing, sill panning, brackets, fasteners or other items.
- \* Dimensions in parentheses are in millimeters or square meters.
- \* For two-panel patio doors with one panel open, clear opening is based on active panel being open and passive panel being closed.



## ENTRY DOORS



Custom-size doors are available in 1/8" (3) increments.

Available in custom designed panels. Stationary doors are also available (i.e. AEDD2068S or AEDD4068SS).

### Rectangular Outswing Entry Door Dimensions and Specifications

Door Number	Number of Panels Open*	Min. Rough Opening										Clear Opening Maximums					Overall Door Area Sq. Ft./(m <sup>2</sup> )
		Width Inches/(mm)		Height Inches/(mm)	Width Inches/(mm)		Height Inches/(mm)	Clear Opening Sq. Ft./(m <sup>2</sup> )	90° Width Inches/(mm)		Full Width Inches/(mm)	Height Inches/(mm)	Vent Sq. Ft./(m <sup>2</sup> )				
AEDD2068	1	25 1/8" (652)	82"	(2083)	26 1/8" (665)	82 1/2" (2096)	12.68 (1.18)	21 1/8" (537)	23 1/8" (586)	79 1/8" (2011)	12.58 (1.17)	14.63 (1.36)					
AEDD2668	1	31 1/8" (805)	82"	(2083)	32 1/8" (818)	82 1/2" (2096)	15.98 (1.48)	27 1/8" (689)	29 1/8" (738)	79 1/8" (2011)	15.82 (1.47)	18.04 (1.68)					
AEDD2868	1	33 1/8" (856)	82"	(2083)	34 1/8" (868)	82 1/2" (2096)	17.08 (1.59)	29 1/8" (740)	31 1/8" (789)	79 1/8" (2011)	16.89 (1.57)	19.18 (1.78)					
AEDD3068	1	37 1/8" (957)	82"	(2083)	38 1/8" (970)	82 1/2" (2096)	19.28 (1.79)	33 1/8" (841)	35 1/8" (891)	79 1/8" (2011)	19.00 (1.77)	21.46 (1.99)					
AEDD3668	1	43 1/8" (1110)	82"	(2083)	44 1/8" (1122)	82 1/2" (2096)	22.58 (2.10)	39 1/8" (994)	41 1/8" (1043)	79 1/8" (2011)	22.13 (2.06)	24.88 (2.31)					
AEDD2080	1	25 1/8" (652)	95"	(2413)	26 1/8" (665)	95 1/2" (2426)	14.76 (1.37)	21 1/8" (537)	23 1/8" (586)	92 1/8" (2342)	14.66 (1.36)	16.95 (1.57)					
AEDD2680	1	31 1/8" (805)	95"	(2413)	32 1/8" (818)	95 1/2" (2426)	18.61 (1.73)	27 1/8" (689)	29 1/8" (738)	92 1/8" (2342)	18.45 (1.71)	20.90 (1.94)					
AEDD2880	1	33 1/8" (856)	95"	(2413)	34 1/8" (868)	95 1/2" (2426)	19.89 (1.85)	29 1/8" (740)	31 1/8" (789)	92 1/8" (2342)	19.69 (1.83)	22.22 (2.06)					
AEDD3080	1	37 1/8" (957)	95"	(2413)	38 1/8" (970)	95 1/2" (2426)	22.45 (2.09)	33 1/8" (841)	35 1/8" (891)	92 1/8" (2342)	22.17 (2.06)	24.86 (2.31)					
AEDD3680	1	43 1/8" (1110)	95"	(2413)	44 1/8" (1122)	95 1/2" (2426)	26.29 (2.44)	39 1/8" (994)	41 1/8" (1043)	92 1/8" (2342)	25.84 (2.40)	28.82 (2.68)					
AEDD4068	2	50 1/4" (1289)	82"	(2083)	51 1/4" (1302)	82 1/2" (2096)	26.46 (2.46)	44 1/8" (1122)	48 1/8" (1222)	79 1/8" (2011)	25.73 (2.39)	28.90 (2.68)					
AEDD4068	1	50 1/4" (1289)	82"	(2083)	51 1/4" (1302)	82 1/2" (2096)	12.65 (1.18)	21" (533)	23" (584)	79 1/8" (2011)	12.28 (1.14)	28.90 (2.68)					
AEDD5068	2	62 1/4" (1594)	82"	(2083)	63 1/4" (1607)	82 1/2" (2096)	33.06 (3.07)	56 1/8" (1427)	60 1/8" (1527)	79 1/8" (2011)	32.38 (3.01)	35.73 (3.32)					
AEDD5068	1	62 1/4" (1594)	82"	(2083)	63 1/4" (1607)	82 1/2" (2096)	15.95 (1.48)	27" (686)	29" (737)	79 1/8" (2011)	15.60 (1.45)	35.73 (3.32)					
AEDD5468	2	66 1/4" (1695)	82"	(2083)	67 1/4" (1708)	82 1/2" (2096)	35.26 (3.28)	60 1/8" (1529)	64 1/8" (1629)	79 1/8" (2011)	34.43 (3.20)	38.01 (3.53)					
AEDD5468	1	66 1/4" (1695)	82"	(2083)	67 1/4" (1708)	82 1/2" (2096)	17.05 (1.58)	29" (737)	31" (787)	79 1/8" (2011)	16.63 (1.54)	38.01 (3.53)					
AEDD6068	2	74 1/4" (1899)	82"	(2083)	75 1/4" (1911)	82 1/2" (2096)	39.66 (3.68)	68 1/8" (1732)	72 1/8" (1832)	79 1/8" (2011)	38.48 (3.57)	42.57 (3.95)					
AEDD6068	1	74 1/4" (1899)	82"	(2083)	75 1/4" (1911)	82 1/2" (2096)	19.25 (1.79)	33" (838)	35" (889)	79 1/8" (2011)	18.65 (1.73)	42.57 (3.95)					
AEDD7068	2	86 1/4" (2203)	82"	(2083)	87 1/4" (2216)	82 1/2" (2096)	46.26 (4.30)	80 1/8" (2037)	84 1/8" (2137)	79 1/8" (2011)	44.37 (4.12)	49.40 (4.59)					
AEDD7068	1	86 1/4" (2203)	82"	(2083)	87 1/4" (2216)	82 1/2" (2096)	22.55 (2.09)	39" (991)	41" (1041)	79 1/8" (2011)	21.60 (2.01)	49.40 (4.59)					
AEDD4080	2	50 1/4" (1289)	95"	(2413)	51 1/4" (1302)	95 1/2" (2426)	30.81 (2.86)	44 1/8" (1122)	48 1/8" (1222)	92 1/8" (2342)	30.08 (2.79)	33.48 (3.11)					
AEDD4080	1	50 1/4" (1289)	95"	(2413)	51 1/4" (1302)	95 1/2" (2426)	14.72 (1.37)	21" (533)	23" (584)	92 1/8" (2342)	14.36 (1.33)	33.48 (3.11)					
AEDD5080	2	62 1/4" (1594)	95"	(2413)	63 1/4" (1607)	95 1/2" (2426)	38.49 (3.58)	56 1/8" (1427)	60 1/8" (1527)	92 1/8" (2342)	37.80 (3.51)	41.40 (3.85)					
AEDD5080	1	62 1/4" (1594)	95"	(2413)	63 1/4" (1607)	95 1/2" (2426)	18.57 (1.73)	27" (686)	29" (737)	92 1/8" (2342)	18.22 (1.69)	41.40 (3.85)					
AEDD5480	2	66 1/4" (1695)	95"	(2413)	67 1/4" (1708)	95 1/2" (2426)	41.05 (3.81)	60 1/8" (1529)	64 1/8" (1629)	92 1/8" (2342)	40.22 (3.74)	44.04 (4.09)					
AEDD5480	1	66 1/4" (1695)	95"	(2413)	67 1/4" (1708)	95 1/2" (2426)	19.85 (1.84)	29" (737)	31" (787)	92 1/8" (2342)	19.43 (1.81)	44.04 (4.09)					
AEDD6080	2	74 1/4" (1899)	95"	(2413)	75 1/4" (1911)	95 1/2" (2426)	46.17 (4.29)	68 1/8" (1732)	72 1/8" (1832)	92 1/8" (2342)	44.99 (4.18)	49.31 (4.58)					
AEDD6080	1	74 1/4" (1899)	95"	(2413)	75 1/4" (1911)	95 1/2" (2426)	22.41 (2.08)	33" (838)	35" (889)	92 1/8" (2342)	21.81 (2.03)	49.31 (4.58)					
AEDD7080	2	86 1/4" (2203)	95"	(2413)	87 1/4" (2216)	95 1/2" (2426)	53.86 (5.00)	80 1/8" (2037)	84 1/8" (2137)	92 1/8" (2342)	51.96 (4.83)	57.23 (5.32)					
AEDD7080	1	86 1/4" (2203)	95"	(2413)	87 1/4" (2216)	95 1/2" (2426)	26.25 (2.44)	39" (991)	41" (1041)	92 1/8" (2342)	25.30 (2.35)	57.23 (5.32)					

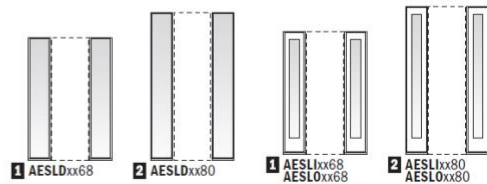
- \* "Door Dimension" always refers to outside frame to frame dimension.
- \* "Minimum Rough Opening" dimensions may need to be increased to allow for use of building wraps, flashing, sill panning, brackets, fasteners or other items.
- \* Dimensions in parentheses are in millimeters or square meters.
- \* For two-panel patio doors with one panel open, clear opening is based on active panel being open and passive panel being closed.

### Direct-Set Rectangular Entry Door Sidelight Dimensions and Specifications

Sidelight Number	Sidelight Dimensions		Min. Rough Opening		Glass Area Sq. Ft. (m²)	Overall Sidelight Area Sq. Ft. (m²)
	Width Inches/(mm)	Height Inches/(mm)	Width Inches/(mm)	Height Inches/(mm)		
AESLD0868	9 1/8" (252)	82" (2083)	10 1/8" (265)	82 1/2" (2096)	3.77 (0.35)	5.66 (0.53)
AESLD1068	15 1/8" (405)	82" (2083)	16 1/8" (418)	82 1/2" (2096)	7.03 (0.65)	9.08 (0.84)
AESLD2068	25 1/8" (652)	82" (2083)	26 1/8" (665)	82 1/2" (2096)	12.32 (1.14)	14.63 (1.36)
AESLD3068	37 1/8" (957)	82" (2083)	38 1/8" (970)	82 1/2" (2096)	18.84 (1.75)	21.46 (1.99)
AESLD0880	9 1/8" (252)	95" (2413)	10 1/8" (265)	95 1/2" (2426)	4.40 (0.41)	6.56 (0.61)
AESLD1080	15 1/8" (405)	95" (2413)	16 1/8" (418)	95 1/2" (2426)	8.19 (0.76)	10.51 (0.98)
AESLD2080	25 1/8" (652)	95" (2413)	26 1/8" (665)	95 1/2" (2426)	14.37 (1.33)	16.95 (1.57)
AESLD3080	37 1/8" (957)	95" (2413)	38 1/8" (970)	95 1/2" (2426)	21.97 (2.04)	24.86 (2.31)

- \* Sidelight Dimension always refers to outside frame to frame dimension.
- \* "Minimum Rough Opening" dimensions may need to be increased to allow for use of building wraps, flashing, sill panning, brackets, fasteners or other items.
- \* Dimensions in parentheses are in millimeters or square meters.

### Direct-Set & Sash-Set Rectangular Entry Door Sidelights



Direct-set (AESLD), sash-set inswing (AESLI) and sash-set outswing (AESLO) entry door sidelights shown. Dimensions and specifications shown for direct-set sidelights, contact your Andersen supplier for sash-set sidelight dimensions and specifications.